THE ASTROPHYSICAL JOURNAL, 414:740–758, 1993 September 10

EVIDENCE FOR A DISPERSION IN THE LITHIUM ABUNDANCES OF EXTREME HALO STARS

CONSTANTINE P. DELIYANNIS[1,2] AND M. H. PINSONNEAULT[3]
Center for Solar and Space Research, Center for Theoretical Physics, and Department of Astronomy, Yale University
AND
DOUGLAS K. DUNCAN[4]
Space Telescope Science Institute
Received 1991 September 30; accepted 1992 December 10

ABSTRACT

Knowledge of the primordial lithium abundance (Li_p) helps to constrain cosmological parameters and to discriminate between models of primordial nucleosynthesis; the best current probe of Li_p is the set of lithium abundances measured in old halo stars, provided that stellar Li depletion mechanisms are taken into account. Standard stellar evolutionary models show little depletion (Deliyannis, Demarque, & Kawaler), consistent with standard big bang nucleosynthesis (BBN), whereas models with rotational mixing deplete about an order of magnitude (Pinsonneault, Deliyannis, & Demarque), possibly consistent with inhomogeneous BBN, or other nonstandard scenarios. One way to test the rotational models is through their prediction that a small dispersion can result in the lithium abundances if there is a significant dispersion in the initial angular momenta. For all available extreme halo dwarf data, we have performed a detailed analysis in the $(b - y)$ color–lithium equivalent width plane, which eliminates many of the uncertainties associated with the transformation to the $T_{\rm eff}$-abundance plane. Furthermore, we have used two independent means to compute the uncertainties: one that incorporates detailed information about the individual S/N and relevant instrumentation, and one that utilizes empirically derived uncertainties from multiple observations; our conclusion is the same in either case. Using χ^2 tests, we find evidence for a small dispersion (of order $\pm 20\%$ about the mean) in the Li equivalent width at fixed color, with a high degree of confidence. Interpreted according to usual standard model atmospheres theory, this translates directly into a small dispersion in the Li abundances themselves. This dispersion is consistent with, but does not uniquely support, the rotational depletion. We have also corrected the colors for reddening, and the evidence for dispersion remains strong. One star, BD 23°3912, lies more than 50% above the lithium plateau.

Subject headings: nuclear reactions, nucleosynthesis, abundances — stars: abundances — stars: Population II

1. INTRODUCTION

Knowledge of the primordial lithium abundance (Li_p) can constrain important cosmological parameters, such as the baryon-to-photon ratio, the baryonic density of the universe, and the number of neutrino families. It can also test the self-consistency of models of primordial nucleosynthesis (Wagoner 1973; Yang et al. 1984; Deliyannis et al. 1989; Malaney & Mathews 1991). The best probe of Li_p currently is the set of lithium abundances measured in old halo stars, *provided that stellar Li depletion mechanisms are taken into account.* The kinematics of old halo stars suggest that, as a group, they sample the protogalaxy well; a consideration of Galactic Li production/destruction mechanisms suggests that the protogalactic Li abundance reflects well Li_p (Rebolo, Molaro, & Beckman [RMB] 1988; Deliyannis 1990; Deliyannis, Demarque, & Pinsonneault 1991).

Spite & Spite (1982) discovered that the hotter halo dwarfs have a nearly constant lithium abundance, with little evidence for any dispersion at fixed $T_{\rm eff}$ or even any dependence on $T_{\rm eff}$. This possibly uniform plateau (at [Li] $\sim$ 2.08[5]) ranges over 800 K in $T_{\rm eff}$; however, the cooler halo dwarfs show progressively more depletion. These properties have been confirmed and extended to cover over 2 orders of magnitude in [Fe/H] (see compilation of sources in Table 1). However, as the kinematic selection criterion is relaxed and especially as the metallicity increases, the observations show progressively more dispersion at a fixed $T_{\rm eff}$ (Deliyannis, Demarque, & Kawaler 1990; hereafter DDK). This pattern complicates the task of interpretation, where differential Galactic Li enrichment is one possible interpretation, and complex stellar depletion from a higher initial abundance is another. In the present work, we will use the definition of DDK for extreme halo stars (the "Group A" stars of DDK), namely those with space motion $|V_{\rm LSR}| \geq 160$ km s^{-1} and [Fe/H] ≤ -1.3 unanimously according to all sources quoted in DDK.

If the extreme plateau stars are interpreted as essentially undepleted in Li, then the standard model of big bang nucleosynthesis (BBN) is remarkably self-consistent (Boesgaard & Steigman 1985; Krauss & Romanelli 1990; Pagel 1991; Deliyannis et al. 1991). Support for this interpretation comes from standard models of stellar evolution, which agree closely with

[1] Now Beatrice Watson Parrent Postdoctoral Fellow at Institute for Astronomy, University of Hawaii.
[2] Present postal addresses: Institute for Astronomy, University of Hawaii, 2680 Woodlawn Drive, Honolulu, HI 96822.
[3] Department of Astronomy, Yale University, P.O. Box 6666, New Haven, CT 06511.
[4] University of Chicago, Department of Astronomy and Astrophysics, 5640 Ellis Avenue, Chicago, IL 60637.

[5] Lithium (and beryllium) abundances are given by number relative to hydrogen on a logarithmic scale where hydrogen is 12, and are represented by notation "[Li]"; i.e., [Li] $\equiv 12 + \log (N_{\rm Li}/N_{\rm H})$. We also employ the usual notation for relating iron abundances to solar values: [Fe/H] = $\log (\rm Fe/H)_* - \log (\rm Fe/H)_{star}$.

TABLE 1

OBSERVED PARAMETERS, EQUIVALENT WIDTHS, AND UNCERTAINTIES

											THEORETICAL σ		EMPIRICAL σ		EMPIRICAL σ	
STAR[a] (1)	OTHER NAMES (2)	SOURCE[b] (3)	[Fe/H] (4)	$b-y$ (5)	$E(b-y)$ (6)	$(b-y)_0$ (7)	S/N[c] (8)	W(Li) (source) (mÅ) (9)	$\sigma_{w(\mathrm{Li})}$ (mÅ) (10)	σ_{other} (11)	W(Li) (2 mÅ min) (12)	σ_w (13)	W(Li) (2.8 mÅ all) (14)	σ_w (15)	W(Li) (2.1 & 3.7 mÅ) (16)	σ_w (17)
19445	25°0495	SS1	−2.2	0.352	0.003	0.349	237[d]	33	0.9[e]	...	35.4	1.3	35.4	1.6	35.4	1.2
		HD	...	...	...	...		38	2	...						
		RMB	...	...	...	...	160	35	2.9	...						
74000	−15°2546	SS3	−1.8	0.311	−0.013	0.324	65	24.5	3.2	...	24.5	3.2	24.5	2.8	24.5	2.1
84937	14°2151	SS1	−2.1	0.303	0.013	0.290	100	18	2.1	...	21.8	1.1	21.5	1.4	20.2	1.3
		B	...	...	...	...	300	23	0.45[e]	...						
		HD	...	...	...	...		20	3	...						
		PHD	...	...	...	...	182	25	0.36[e]	...						
108177[f]	2°2538	SS2	−1.9	0.330	0.004	0.326	30	35	6.8	...	29.5	1.9	29.5	2.0	29.5	2.1
		SS3	...	...	...	...	150	29	1.4[e]	...						
132475	−21°4009	RMB	−1.6	0.401	0.046	0.355	110	52	4.3	...	52	4.3	52	2.8	52	2.1
140283	−10°4149	SS1	−2.5	0.380	0.020	0.360	241[d]	45	0.85[e]	...	46.6	1.5	46.6	1.6	46.6	1.2
		HD	...	...	...	...		48	3							
		RMB	...	...	...	...	130	50	3.6							
160617	−40°11755	SS3	−1.6	0.347	0.059	0.288	100	42	3.8	...	42	3.8	42	2.8	42	2.1
194598	9°4529	SS1	−1.6	0.344	−0.006	0.350	300	27	0.69[e]	...	27	2.0	27	2.8	27	2.1
219617	−14°6437	SS1[g]	−1.4	0.349	−0.001	0.350	200	42	1.0[e]	...	41.8	1.5	41.8	1.6	41.8	1.2
		HD	...	...	...	...		43	3							
		RMB	...	...	...	...	150	40	3.1							
−10°388	G271−162	RMB	−2.4	0.326	0.024	0.302	100	35	4.7	...	29.1	1.8	31.5	2.0	32.0	1.8
		HT	...	...	...	...	>100[h]	28	2.0	2						
2°3375	G20−8	RMB	< −2.5	0.356	0.006	0.350	110	30	4.3	...	30	4.3	30	2.8	30	2.1
2°4651	G29−23	SS2	−2.3	0.339	0.012	0.327	100	27	2.1	...	27	2.1	27	2.8	27	2.1
3°740	G84−29	RMB	−2.9	0.312	0.019	0.293	100	21	4.7	...	17.6	1.8	19	2.0	20	1.8
		HP	...	...	...	...	160	17	1.3[e]	1.5						
9°352	G76−21	RMB	−2.2	0.345	0.020	0.325	70	34	6.7	...	34	6.7	34	6.0	34	6.0
17°4708	G126−62	HD	−1.8	0.330	0.000	0.330	...	25	1.5[e]	...	25	1.7	25	2.0	25	1.5
		RMB	...	...	...	...	130	25	3.6	...						
20°3603	G183−11	SS1	−2.2	0.319	0.010	0.309	70	28	2.9	...	27.5	2.1	27.5	2.0	27.5	1.5
		HD	...	...	...	...	...	27	3							
21°607	HD 284248	SS2	−1.6	0.328	−0.006	0.334	80	25	2.6	...	25	2.6	25	2.8	25	2.1
24°1676	G88−32	HT	−2.6	0.311	0.003	0.308	>100[h]	26	2.0	2	26	2.8	26	2.8	26	3.7
26°2606	G166−45	RMB	−2.9	0.336	0.025	0.311	160	35	2.9	...	30.9	1.6	32	2.0	33.5	1.8
		HT	...	...	...	...	>100[h]	29	2.0	2						

1993ApJ...414..740D

TABLE 1—*Continued*

Star[a] (1)	Other Names (2)	Source[b] (3)	[Fe/H] (4)	$b-y$ (5)	$E(b-y)$ (6)	$(b-y)_0$ (7)	S/N[c] (8)	W(Li) (source) (mÅ) (9)	$\sigma_{w(Li)}$ (mÅ) (10)	σ_{other} (11)	Theoretical σ: W(Li) (2 mÅ min) (12)	Theoretical σ: σ_w (13)	Empirical σ: W(Li) (2.8 mÅ all) (14)	Empirical σ: σ_w (15)	Empirical σ: W(Li) (2.1 & 3.7 mÅ) (16)	Empirical σ: σ_w (17)
29°2091	G119−32	RMB	−2.1	0.377	0.002	0.375	70	45	6.7	...	45	6.7	45	6.0	45	6.0
34°2476[f]	G165−39	SS3	−2.3	0.309	0.007	0.302	100	22	2.1	...	22.5	1.4	22.5	2.0	22.2	1.8
		HP	...	...	...	...	110	23	1.8[e]	2						
42°2667	G180−24	RMB	−1.7	0.340	−0.007	0.347	100	28	4.7	...	28	4.7	28	2.8	28	2.1
59°2723	G217−8	RMB	−1.6	0.330	0.009	0.321	80	25	5.8	...	25	5.8	25	6.0	25	6.0
72°94	...	RMB	−1.8	0.309[i]	...	...	80	27	5.8	...	27	5.8	27	6.0	27	6.0
G4−37.....	...	HT	−2.7	0.363	0.064	0.299	85	20	2.5	2	20	2.5	20	2.8	20	3.7
G48−29	LP 608−62 1°2341p	HD	−2.7	0.299	0.008	0.291	...	23	4.5	...	23	4.5	23	3.4	23	4.5
G59−24	...	HT	−2.6	0.332	−0.004	0.336	60	34	3.4	3	34	3.4	34	2.8	34	3.7
G64−12	...	RBM	−3.5	0.312	0.034	0.278	100	23	4.7	...	24.0	3.3	24	2.0	24	2.6
		SSPC	...	...	...	...	40	25	4.6							
No $(b-y)$																
G201−5	...	HT	−2.7	...	...	...	>100[h]	25	2.0	(2)	25	2.0				
G238−30 ...	...	SSPC	−3.0	...	...	...	40	33	4.6	...	33	4.6				
Less Extreme																
23°3912	...	SS2	−1.5	0.372	0.013	0.359	130	67	1.6[e]	...	68.7	1.7	70	2.8	70	2.1
		RMB	...	...	...	...	150	73	3.1							

[a] HD, BD, or G number.

[b] SS1: Spite & Spite 1982; SS2: Spite, Maillard, & Spite 1984; SS3: Spite & Spite 1986; HD: Hobbs & Duncan 1987; SSPC: Spite et al. 1987; RBM: Rebolo, Beckman, & Molaro 1987; RMB: Rebolo, Molaro, & Beckman 1988; HP: Hobbs & Pilachowski 1988; PHD: Pilachowski, Hobbs, & De Young 1989; HT: Hobbs & Thorburn 1991.

[c] HD do not list individual S/N: however, they do give uncertainties in W_{Li}. These are 2 σ uncertainties (L. M. Hobbs 1991, private communication), so we list half their uncertainties in col. (10). Also, see the note at the end of SS1 for the values of S/N we quote from their paper.

[d] The source in col. (3) lists individual S/N for each night, but only the combined W_{Li}. We thus list the combined S/N from all nights, derived by adding in quadrature the S/N from each night.

[e] The value 2 mÅ has been used in computing col. (12). See text (§ 2.1).

[f] HD list an upper limit in W_{Li} for this star. We ignore this, and consider the detections listed in col. (9) as superceding. See also discussion in DDK (§ 4.2).

[g] SS3 use this star as a comparison star between CFHT and CASPEC, and report W_{Li} = 40 mÅ, which is in good agreement with the other values listed in col. (9); since no S/N is given, we ignore this report.

[h] HT do not give a precise value for S/N, but indicate S/N > 100. To be conservative, we assume S/N = 100.

[i] We could not find a reddening for this star, so we have assumed a value of $E = 0$. Since this star is already located above the mean trend regardless of whether the fit is derived with or without reddening for the other stars, *any* amount of reddening that this star might have would further strengthen the case for dispersion.

the depleted cool dwarfs, the plateau stars, and the diluting subgiants (DDK), but imply only a slightly higher initial abundance (Li_i) for these stars ([Li] ~ 2.17). Note that even in this case, the success of standard BBN is marginal (though remarkable), owing to currently accepted estimates for the primordial helium abundance (Y_p); a slightly lower Y_p would point to an inconsistency.

However, it is possible that physical mechanisms that are not usually considered in standard models, such as rotationally induced mixing, might cause significant depletion. This possibility is especially relevant since standard stellar models cannot reproduce the lithium depletion seen in open clusters (Pinsonneault, Kawaler, & Demarque 1990), or even in the Sun. The recent evolutionary models of Pinsonneault, Deliyannis, & Demarque (1992; hereafter PDD) have considered a large variety of instabilities (including circulation) that might cause rotationally induced mixing, and demonstrate that halo dwarfs could have depleted their Li by as much as an order of magnitude.[6] If this is correct, the implications for BBN would be profound: the standard model would no longer be self-consistent, and some variant would be required. In fact, the combination of a slightly lower Y_p and/or higher Li_p (but not necessarily a full order of magnitude) would point to an inconsistency. Some possible variants (massive neutrinos, inhomogeneities) are discussed in Deliyannis et al. (1991).

It is thus crucial to identify observational tests that might be able to differentiate between the two scenarios or point to some third scenario or combination. To this end, DDK defined a series of requirements that successful models (e.g., with different physical assumptions) must meet. These include reproduction of the nearly flat Spite plateau for the hotter dwarfs and the observed depletion for the cooler dwarfs, again the flat plateau for the near-turnoff subgiants and the observed depletion (due minimally to dilution) for the cooler subgiants, at most a small dispersion for the extreme halo dwarfs, and more dispersion for more metal-rich stars. Both standard models (DDK) and rotational models (PDD) reproduce well the morphology of the Li observations.[7] A possible differentiating test is the prediction of rotational models that halo stars should have a small dispersion in Li abundances due to differences in the initial angular momenta. (Note that Population I models produce a larger dispersion, which is observed in Population I clusters.) However, note also that dispersion in the halo stars can conceivably be created by localized Galactic Li enrichment as well. Thus, while the complete absence of intrinsic dispersion in the halo dwarf Li abundances would argue against the rotational models, the presence of a small dispersion would be consistent with the models, although it would not necessarily confirm them.

[6] Rotational Population I models also deplete Li, so that Galactic Li enrichment is still required in this picture.

[7] Another class of models, those that include the effects of microscopic diffusion (Michaud, Fontaine, & Beaudet 1984; DDK) have also been subjected to this test. Claims that diffusion can raise Li_p to 2.5 (Proffitt & Michaud 1991) are exaggerated because such models do not reproduce the morphology of the Li observations (Deliyannis & Demarque 1991b). More recent models are better able to match the observations (Chaboyer et al. 1992), in part because of the use of improved model physics. Diffusion preferentially depletes the hot edge of the Spite plateau, so by necessity, models that are consistent with the observations are ones that have not suffered much diffusion. Chaboyer et al. find $Li_p \sim 2.24$ for diffusive models, which is only slightly higher than the value of DDK derived from standard models (2.17). Thus, the implications for BBN from successful diffusive stellar models are nearly indistinguishable from those of standard stellar models.

A first glance at the halo dwarf lithium observations in the Spite plateau suggests that they are remarkably uniform, with a maximum possible variation of a factor of 2 at ~5800 K. Is part of this variation a reflection of an intrinsic dispersion, or is it just a result of the observational uncertainties? DDK calculated a standard deviation σ of 0.09 dex in [Li] for the data in the usual Li–$T_{\rm eff}$ plane. Given the observers' relative uncertainty of 0.10–0.11 dex, this σ is statistically consistent with a perfectly uniform distribution. Furthermore, each of the three major studies employed different instrumentation, assumptions, and model atmospheres. Thus, even for an intrinsically uniform distribution, the combined data might be expected to yield a larger (not smaller) σ than the quoted relative uncertainty. If the stars possess an intrinsic dispersion, the σ should be larger still. However, it is not inconceivable that a small intrinsic dispersion could be hidden within the sample of 24 plateau stars.

An improved analysis can be performed in the equivalent width–color plane; the purpose of this paper is to test the possibility that a dispersion might exist in the Li abundances of extreme halo plateau dwarfs using the $W_{\rm Li}$–color plane. Avoiding the transformation from the $W_{\rm Li}$–color plane to the Li–$T_{\rm eff}$ plane (i.e., from observed equivalent widths to derived abundances and from observed colors to derived surface temperatures) eliminates uncertainties, both random and systematic, in the model atmospheres themselves and in the parameters that are used as input for the model atmospheres. However, there still exist uncertainties in $W_{\rm Li}$ and in color that must be considered carefully. Although detailed uncertainties in $W_{\rm Li}$ have not been presented in most of the sources listed in Table 1, we derive uncertainties in $W_{\rm Li}$ using two independent and complementary means: First, we use the expression for σ_W derived in Cayrel (1988) to calculate individual σ_W from knowledge of the signal-to-noise ratio (S/N) of each observation, and the instrumentation used by each source (§ 2). Second, we make empirical assessment of the uncertainties in the $W_{\rm Li}$, using independent measurements of the same stars (§ 2). Reassuringly, our conclusions will not depend on which means is used to determine the uncertainties in the $W_{\rm Li}$.

Uncertainties in the color are also important: The observed lithium abundances are derived from the Li I resonance line at 6708 Å. The fraction of neutral lithium varies across the plateau because lithium is easily ionized. As a result, for a constant abundance the equivalent width of the line decreases for hotter stars which have less neutral lithium. The measured equivalent width is thus a strong function of color. For an improved analysis, it is therefore also essential to have a uniform set of photometry to minimize relative errors in the color. The excellent and extensive photometric survey of halo stars of Schuster & Nissen (1988, 1989a, b; hereafter SN1, SN2, SN3) provide such a uniform set (§ 2). In § 3 we test for dispersion by performing a χ^2 analysis.

We also discuss the uncertainties due to reddening, which have usually been ignored in the past since most relevant halo dwarfs are nearby. We will see that reddening can be important for some stars, mostly the more distant ones in the sample. However, reddening does not affect our conclusion that a small but real dispersion in Li abundances seems to be present.

2. DERIVATION OF UNCERTAINTIES

In this section we derive and discuss uncertainties for the equivalent widths (§ 2.1), and discuss uncertainties in the color (§ 2.2), uncertainties due to reddening (§ 2.3), and other possible uncertainties (§ 2.4).

2.1. Li *Equivalent Widths*

We will employ two independent and complementary methods, each with its own advantages, to estimate uncertainties in the equivalent width. The first method estimates the expected random errors based on the individual S/N attained for each observation and the instrumentation used (§ 2.1.1). A possible advantage of this approach is that it may be able to identify the more reliable measurements and put more weight on them; a possible disadvantage may be manifest in the difficulty of identifying the importance and magnitude of systematic errors. The second method estimates the total error by comparing pairs of observations of the same stars (§ 2.1.2). While this method may estimate a typical error more realistically, it might be more difficult to identify (and weight appropriately) which measurements are more reliable. Fortunately, our conclusions will be the same using either method.

2.1.1. *Theoretically Derived Random Errors*

Table 1 contains nearly all the lithium equivalent widths available for normal extreme dwarfs at the time of submission of this paper,[8] for a total of 30 stars, and summarizes the data we have used. Column (1) gives the star name (HD or BD except where noted), and column (2) gives alternate names. Column (3) shows the source for columns (8), (9), and (11); note that abbreviations for each source are defined in note b. Column (4) lists the averaged metallicity from the sources quoted in DDK and/or the sources listed in column (3). Columns (5) and (6) give the color $(b-y)$ and reddening $E(b-y)$ of SN1 and SN3 for each star (see § 3.2), and column (7) gives the dereddened $(b-y)_0 = (b-y) - E(b-y)$. Column (8) gives the S/N for each observation, and column (9) the measured equivalent width.

For a given observation, the random uncertainty which can be expected theoretically in the derived equivalent width depends on the S/N for that observation, on the (effective) resolution of the spectrograph (given by standard width s or the full width at half maximum $F \sim 2.354$ s), and on the effective pixel size d (e.g., Cayrel 1988)

$$\sigma_W = K\epsilon ,$$

where

$$K = \sqrt[4]{9\pi}\sqrt{sd} \sim 1.503\sqrt{Fd} \qquad (1)$$

depends only on the instrumentation, and $\epsilon \equiv (\mathrm{S/N})^{-1}$. (Table 2 shows the instrumentation parameters of each observing group, and their factor K.) In column (10) of Table 1 we give the random 1 σ uncertainty that we derive for each W_{Li} using equation (1) (except for source HD, see note c in Table 1). For comparison, column (11) shows the σ_w derived independently by Hobbs & Pilachowski (1988) (HP) and Hobbs & Thorburn (1991) (HT). In fact, the values in column (11) agree well with our values in column (10). We have not yet included possible systematic errors (e.g., in the placement of the continuum, the flat-fielding, the background subtraction, the dark current subtraction, light scattering in the spectrograph), nor indeed can we do so directly since the information is not available to us(!), but there are reasons to believe that for most stars these are relatively small.

Cayrel (1988) finds that systematic effects become important when the random error is calculated to be less than 1 mÅ and that repeated measurements yield a scatter of 1–2 mÅ in such cases and suggests that the primary source for additional error generally is in the placement of the continuum. (For five out of 45 total measurements in the sample of 30 stars, the derived σ_W in col. [9] are indeed less than 1 mÅ.) Spectra of (metal-poor) halo plateau dwarfs are relatively uncrowded near the Li I line, so that the accuracy in placing the continuum should improve with higher S/N. We shall attempt to include possible systematic errors by adopting a 2 mÅ minimum uncertainty: for every observation where the calculated random error is less than 2 mÅ (this happens for 10 out of the 45 measurements), we will assume a total uncertainty of 2 mÅ, and we will assume that the random uncertainty dominates in the other observations. It can be argued (as above) that the minimum total uncertainty ought to be smaller, perhaps between 1 and 2 mÅ, but we prefer to be conservative and err on the side of overestimating the errors.

Columns (12) and (13) show the weighted mean equivalent width and resulting standard deviation for each star, assuming a minimum uncertainty of 2 mÅ for each observation.

2.1.2. *Empirically Derived Total Errors*

At high S/N levels other small systematic effects are often seen in detectors, and in that case the theoretical maximum accuracy is not fully achieved. Fortunately, in the present instance we have enough independent measurements of the same stars that an assessment of measurement error can be made independently of theoretical considerations. There are 23 pairs of independent measurements of the same stars listed in Table 1. Since they are made with completely different telescopes and detectors, at different times, they should reveal the effects of all sources of error affecting the equivalent width determinations. The rms difference shown by these pairs is 3.95 mÅ. If one assumes equal uncertainty in all measurements, an error of 2.8 mÅ *per measurement* is indicated. There is an indication that some measurements are better than others. Over half the pairs come from three sets of measurements by SS1–3, HD, and RMB (cf. notes to Table 1 for references). This "primary sample" may be analyzed separately, and the 12 pairs show rms differences of 2.9 mÅ, indicating an uncertainty of 2.1 mÅ per measurement. Pairs involving any of the other measurements show an rms difference of 5.3 mÅ, suggesting an average uncertainty of 3.7 mÅ measurement.

HD performed their own assessment of their errors of measurement. The values they list for five stars which are members of the pairs analyzed above average 2.6 mÅ, in excellent agreement with the independent estimate derived here. A further check is provided by the star HD 84937, which was measured independently four times. The rms scatter of those measurements is 3.1 mÅ, or 2.2 mÅ per measure, again in excellent agreement with the uncertainties derived here. It can thus be argued that the uncertainty in the equivalent width is well determined. In addition to the case of theoretically determined errors above (§ 2.1.1), we will analyze the data considering two

[8] There exist a few additional observations that are not considered here. For example, see Hobbs, Welty, & Thorburn (1991) for an example of a hot halo dwarf with significantly depleted lithium. Although this star would support the case for dispersion, we do not consider it here because it may not be a normal star. Hobbs et al. (1991) suggest that (among other possibilities) it may be a field "blue straggler." Other halo "blue stragglers" also show anomalously low Li abundances (Hobbs & Duncan 1987 [HD]; Hobbs & Mathieu 1991). There is also the case of CS 22876−32, the most metal-poor known dwarf with [Fe/H] = −4.3, in the middle of the plateau ($T_{\mathrm{eff}} \sim 5900$), might also have depleted Li (Molaro 1991). In addition to the 30 Group A stars that we consider, we do include one star, BD 23°3912 (see last entry in Table 1), which satisfies the metallicity criterion of the "extreme halo" but is slightly outside the kinematic cutoff. This star is discussed separately below.

TABLE 2

INSTRUMENTATION AND RESULTING K FACTOR

Study (1)	Telescope (2)	Reciprocal Dispersion[a] (Å mm^{-1}) (r_d) (3)	Physical Pixel (Diode) Size (mm)[a] (x_p) (4)	Effective Pixel Size (mÅ pixel^{-1}) (d) (5)	Source[b]	Resolving Power[a] (R) (6)	Resolution (FWHM) (mÅ) (F) (7)	Source[b,c]	K (mÅ) (K) (8)
SS1, SS2	CFHT	4.8	0.015	72	DPD, p1	...	260	(1)	206
SS3[d]	CFHT	4.8	0.015	72	DPD	40,000	260	c1	206
SS3[e]	ESO–CASPEC	6	0.030	180	DPD, p1	20,000	360	DPD, p1	383
SSPC	MMT	...	...	62	c2	...	250	(1), c2	187
RMB, RBM ...	Newton	9.8	...	220	(1)	...	440	c3, p2	468
B	CHFT	...	0.015	72	DPD, p3	...	112	(1)	134
HT, HP	KPNO 4m	6.33[p4]	0.015[p4]	95	p4	...	190	p4	202
PHD	KPNO 2.1 m	1.93[b]	0.015	29	(1)	105,000	64	DPD	64.8

[a] Source is the study(ies) in col (1), unless noted otherwise.

[b] Source for col. (5): DPD derived here using either $r_d \cdot x_p = d$, or $R \cdot F = \lambda = 6708$ Å; p1–p4: private communication (see below); c1–c3: see below; (1): study(ies) in col. (1).

[c] For several observations we have chosen to be more conservative than might be necessary, possibly overestimating the value of K (and thus σ_W). If smaller σ_W are indeed more appropriate in these cases, then the conclusion that there is a dispersion would follow at slightly higher confidence limits. The relevant observations are as follows (notes c1–c3).

[c1] We have used the value 0.26 Å of SS1 and SS2. However, SS3 state a resolving power of 40,000; if this is taken at face value, then the FWHM resolution is finer, at 167 mÅ. This would reduce our derived σ_W by 20% for the observations of SS3 for HD 74000, HD 108177, and BD 34°2476.

[c2] It is not clear that eq. (1) applies well to this observation. The spectrograph at the MMT has high resolution, but is noisy, so a filtering was used about "4 pixels wide," yielding a line that was 250 mÅ wide; regardless, it seems likely that if anything, we have overestimated the (effective) value of K (M. Spite 1991, private communication).

[c3] Rebolo has indicated 440 mÅ or "slightly less" (R. Rebolo 1991, private communication), which we adopt, to be conservative. Note that taking the resolving power of RMB of 20,000 yields FWHM = 360 mÅ, and RBM state FWHM = 0.4 Å.

[d] For all their stars except HD 160617 and HD 166913 (the latter is not used here because DDK found it to have evolved past the turnoff).

[e] For HD 160617. Note that $F = 360$ is based on $R = 19{,}000$ (M. Spite 1991, private communication).

[p1] M. Spite 1991, private communication.

[p2] R. Rebolo 1991, private communication.

[p3] A. M. Boesgaard 1991, private communication.

[p4] L. M. Hobbs 1991, private communication.

cases of the empirically determined errors: one case with 2.8 mÅ accuracy for each independent measurement (see cols. [14] and [15] of Table 1 for the weighted mean equivalent width and resulting standard deviation for each star), and another case with 2.1 mÅ accuracy for each measurement of the "primary sample" and 3.7 mÅ accuracy for each of the other measurements (see cols. [16] and [17] of Table 1 for the weighted mean equivalent width and resulting standard deviation for each star). Either characterization of the errors will turn out to produce similar results. In a few cases where the theoretically expected accuracy is worse than this (due to low S/N and only a single measurement available), a lower accuracy is adopted.

2.2. *Color*

The survey of SN1 includes all but two (G201−5 and G238−30) of the extreme stars, and BD 23°3912. Furthermore, this data set is of excellent quality: the data were obtained with a multichannel photoelectric photometer which obtains simultaneously each of the Strömgren indices, and there are typically several repetitions of each star. For the stars discussed here, SN obtained an "internal mean plus external" uncertainty in $b-y$ of less than 0.005 mag. Keeping in mind that the typical uncertainty may actually be less, and preferring to err on the side of caution, we conservatively take 0.005 as a typical "1 σ" uncertainty in our calculations (for the three faintest stars, G4−37, G59−24, and G64−12, that have $11.1 \leq V \leq 12.0$, the uncertainty may be as large as 0.008); the importance of this value of 0.005 mag is discussed below.

A semi-independent check of the accuracy of the SN1 photometry can be made by comparing their $b-y$ and beta measurements. Both these indices are functions of temperature ($b-y$ is also affected by metallicity and reddening, cf. below), and in a group of unreddened stars of similar metallicity they should be well correlated. Plotting one against the other (Fig. 1) for stars with [Fe/H] ≤ -1.7 and $|E(b-y)| < 0.015$ (a total of 14 stars) reveals a scatter $\sigma = 0.0086$. Uncertainties in both $b-y$ and β contribute to this scatter; we assume that

$$\sigma = \sqrt{(m\sigma_\beta)^2 + \sigma_{b-y}^2},$$

where m is the slope of the fit. If the ratio in the upper limit errors holds also for typical errors (i.e., if $\sigma_\beta/\sigma_{b-y} =$

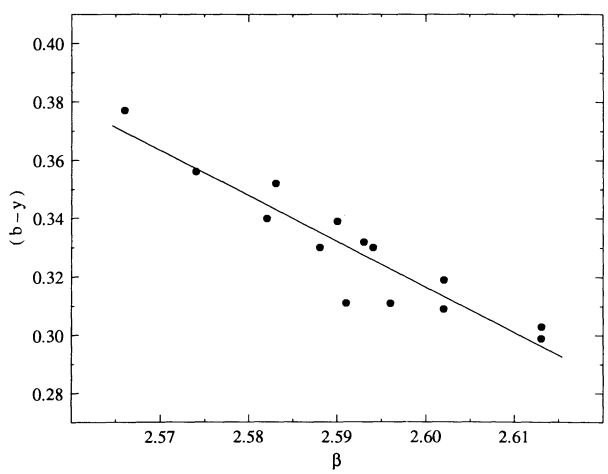

FIG. 1.—$b-y$ and β measurements of SN1

0.008/0.005), then the scatter of 0.0086 translates into typical errors of 0.003 and 0.005 in $b-y$ and β (which is *smaller* than the stated upper limits of SN; reversing the axes in Figure 1 and repeating the analysis yields similar results).

2.3. *Reddening*

Most studies of Li in halo stars have ignored any possible correction in the colors due to reddening, on the basis that nearby (and in many cases high-latitude) stars do not need such corrections: indeed, this is a reasonable assumption for most stars. (Also, detailed reddening estimates do not abound in the literature for single stars.) However, on the basis of interstellar Na I absorption, HT found that a relatively sizable reddening correction applies to G4−37. Without this correction, the derived abundance would fall below the plateau (see Fig. 2*a*). The photometry of Schuster & Nissen indicates sizable reddening for a few other stars as well. SN have estimated reddenings for individual stars using Strömgren *uvbyβ* photometry, and in particular a calibration between the β index and $b-y$ color derived from nearby unreddened stars. Their derived $E(b-y)$ values are listed in column (6) of Table 1; see § 3.2. Reddening, even if small, contributes to the uncertainty in the color, and thus affects the strength of our conclusions regarding a possible dispersion. We will see that even when employing conservatively large estimates for the reddening uncertainty we still find evidence for a dispersion.

2.4. *On Other Possible Uncertainties*

In this section we comment on the possibility that, for a constant Li abundance, other parameters might induce a dis-

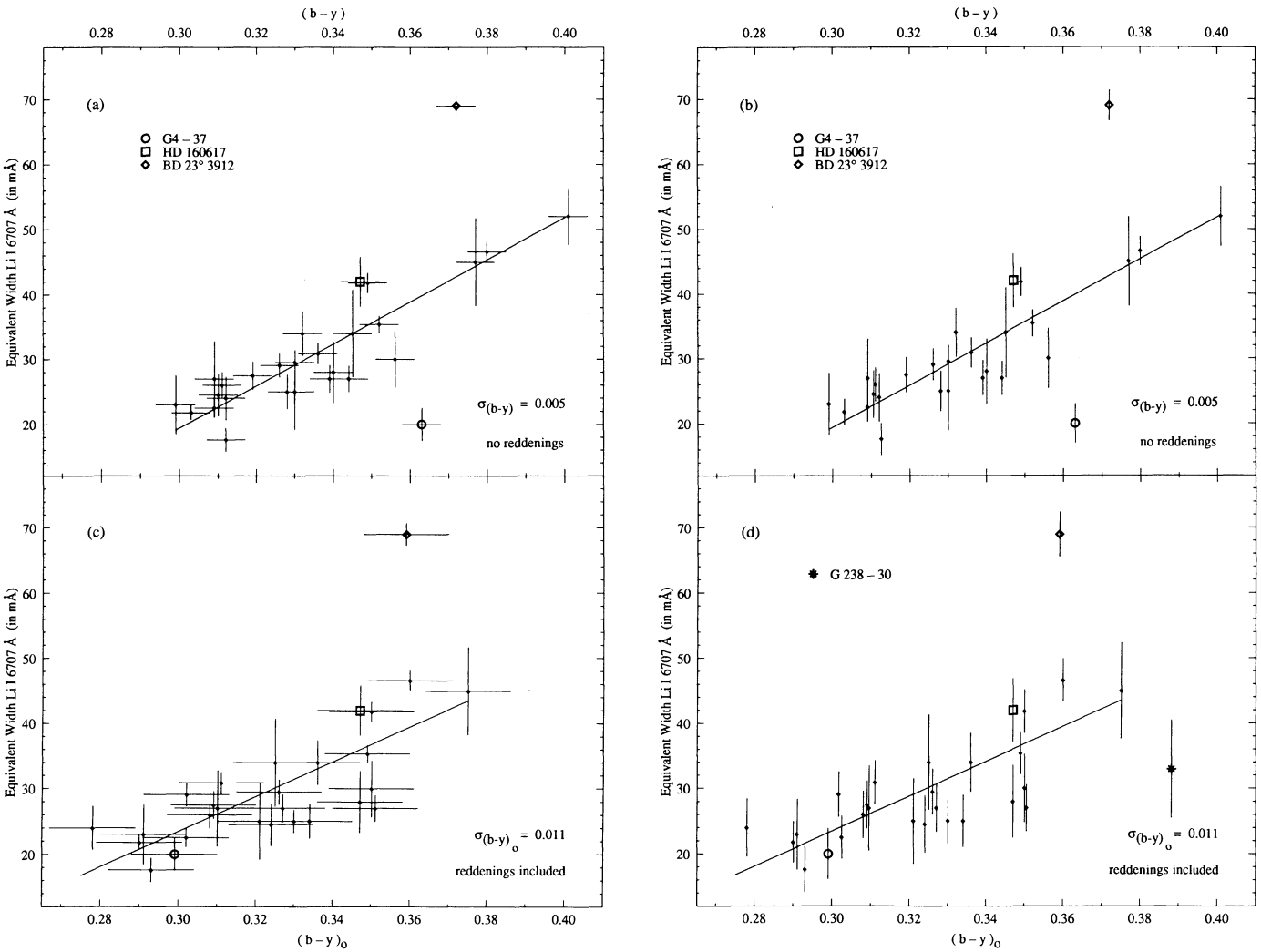

FIG. 2.—$(b-y)$ color vs. lithium equivalent width for extreme halo dwarfs (see Table 1 for sources of observations, and § 3 for analysis). Solid lines show weighted least-squares fits to the observations. In *c* and *d*, *the vertical error bars,* $\sigma_W(tot)$, *include contributions from both* $\sigma_{(b-y)}$ *and* σ_W (*see* § 3.1). The contribution of $\sigma_{(b-y)}$ to σ_W(tot) can thus be inferred by comparing *a* to *b* and *c* to *d*.

(*a*) and (*b*) show the $(b-y)$ colors of SN1, uncorrected for reddening, with assumed $\sigma_{(b-y)} = 0.005$, vs. the weight-averaged W_{Li} derived in col. (11) of Table 1, with σ_W as derived in col. (12) of Table 1. Special symbols have been used for G4−37, which seems to be below the mean trend, for HD 160617 (see text), and for BD 23°3912, which appears above the mean trend. The fit (*solid line*) excludes G4−37 and BD 23°3912 (case 4d in Table 4A, and Table 4D).

(*c*) and (*d*) show $(b-y)_0$, dereddened from $(b-y)$ using $E(b-y)$ from SN2 and SN3, with assumed $\sigma_{E(b-y)} = 0.010$ and $\sigma_{(b-y)} = 0.005$ contributing to $\sigma_{(b-y)_0}$; HD 132475 is not plotted (see § 3.2). G4−37 no longer appears below the mean. The fit (*solid line*) excludes BD 23°3912 and HD 132475 (case 4j in Table 4A, and Table 4J). The star G238−30 is shown only for illustrative purposes (see footnote 14).

persion in the Li equivalent width at fixed color. For example, the range in [Fe/H] and uncertainties in log g could in principle contribute to the scatter in W_{Li} versus $(b-y)_0$; these are discussed below. We will show that, according to model atmospheres, and also from observational evidence (e.g., active stars, also discussed separately below), such scatter seems negligible. Therefore, unless model atmospheres are incomplete with regard to this issue (which is possible), a significant dispersion in W_{Li} at fixed $(b-y)_0$ implies a dispersion in Li abundance.

We do not attempt to quantify other additional possible uncertainties, such as due to microturbulence, macroturbulence, rotation, or magnetic fields, but it is reasonable to suppose that in our *differential analysis* of a sample of rather similar extreme halo dwarfs, such uncertainties may be negligible. In particular, these asymptotically old stars probably all rotate slowly and similarly microturbulence only has a small influence on $b-y$ (Conti & Deutch 1966), and anyway is small in these stars. For completeness it should also be noted that an unknown parameter is apparently inducing color differences in a few of the (many) open clusters measured by Nissen (1988), mostly from cluster to cluster. However, we emphasize that although our stars may span ranges in age and metallicity, they are all old and their *absolute* metal content is always small. Stellar models indicate that their full mass range is less than 0.15 solar masses, and that their structural properties are similar (e.g., DDK). Finally, it is conceivable that chemical peculiarities might affect the $b-y$ color. Two stars in our sample of approximately similar iron abundance, HD 160617 and HD 74000, are significantly nitrogen-rich, with [N/Fe] ~ 2 for both (Bessell & Norris 1982). However, while the former lies above the mean $W_{Li}-(b-y)$ trend, the latter lies on or just below it (Fig. 2); thus it might appear that systematic effects (if any) of excess N on $b-y$ are not important.

2.4.1. [Fe/H]

Intermediate-band colors such as Strömgren b and y are affected by metallicity,[9] and this could in principle confuse relationships in the W_{Li}–color plane. However, our sample is restricted to very metal poor stars where the color effects are small. For example, the theoretical models of VandenBerg & Bell (1985) predict a change in $b-y$ of about 0.025 as metals decline from solar to zero; however, over 80% of that (depending on T_{eff}) occurs as [Fe/H] goes from 0 to -1.0, and (by interpolating) over 90% as [Fe/H] goes from 0 to -1.3. The empirical calibration of Magain (1987), namely

$$b - y = (8330 - T)/[7040(1 - 0.099 \times 10^{[Fe/H]})] , \quad (2)$$

yields slightly larger changes (see Table 3). Even so, for a sample where the metallicity is always below [Fe/H] $= -1.3$, the total expected range due to metallicity variation is only 0.002 at 5500 K and 0.001 at 6300 K. These numbers are negligible compared to our assumed σ_{b-y} of 0.005, and especially compared to $\sigma_{(b-y)_0}$ of 0.011 (see § 3.2). We emphasize that these numbers represent the star-to-star variation due to metallicity, not the total effect. It does not matter that all of the stars have different colors than Population I stars of the same T_{eff}, since we are performing a differential comparison among only metal-poor stars.

[9] $b-y$ is less sensitive to metallicity than $B-V$ primarily because of the longer effective wavelength of the b band compared to B, and because b is narrower, thus not extending far enough into the UV to be affected by the numerous atomic lines there.

TABLE 3

DEPENDENCE OF $b-y$ COLOR ON [Fe/H] (MAGAIN 1987)

T_{eff} (1)	[Fe/H] (2)	$b-y$ (3)
5500	0	0.446
5500	−1.0	0.406
5500	−1.3	0.404
5500	−2.0	0.402
5500	−3.0	0.402
6300	0	0.320
6300	−1.0	0.291
6300	−1.3	0.290
6300	−2.0	0.289
6300	−3.0	0.289

Equivalently, F. Spite (1991, private communication) has kindly calculated for us that at fixed color ($T_{eff} = 6000$ K), going from [Fe/H] $= -1.7$ to -2.7 results in a change of calculated W_{Li} from (e.g.) 21.6 to 21.3 for log $g = 3$ (i.e., less than 1.5% change) and from 22.5 to 22.4 for log $g = 4$ (less than 0.5% change), both of which are negligible.

We can also examine the observations directly and search for systematic effects with metallicity. We have binned the stars into four metallicity groups, with ranges from -1.3 to 1.8, from -1.8 to -2.3, from -2.3 to -2.8, and less than -2.8. We have plotted the bins separately (Figures 3*a*–3*d*) and compared each plot to the same fit derived for all the stars (we have used the fit from Table 4J, which assumes 2 mÅ minimum error, includes reddening, and excludes [see § 3.2] stars HD 132475 and BD 23°3912. HD 132475, for which the reddening is uncertain [see § 3.2], has been plotted with its $b-y$ color; any amount of reddening would move it to the left). No strong systematic effects with metallicity are evident, including in the highest metallicity bin where such effects are expected to be most prevalent, as in fact in each plot the stars appear to be randomly distributed about the general fitting function (see also § 4.2). This conclusion, *if borne out by a larger sample of stars*, may have more general implications as well, such as placing restrictions on models (e.g., stellar depletion, or Galactic Li enrichment) that give different results for the higher metallicity bin than for the lower metallicity bins (§ 4).

2.4.2. *Log g*

A difference in log g from 4.5 to 3.5 can theoretically induce a change in $b-y$ in some cases as large as 0.015 (e.g., F. Spite 1991, private communication). In this study, uncertainties in log g ought to be much smaller than 1 dex. The largest possible ambiguity arises when a post-turnoff star is mistaken for a pre-turnoff star and vice versa, especially toward the cool portion of the plateau. However, DDK separated the dwarfs from the subgiants, using parallaxes. For most stars the separation was clear, especially for the cooler stars, and to be conservative, those stars for which the separation was not clear have not been included in the dwarf sample. Thus, errors of order 1 dex in log g are probably excluded. Let us now determine how much error there might be on the main sequence. Considering ranges of $Y = 0.2$–0.3 to allow (generously!) for the uncertainty in Y, T_{eff} from 5500 to 6300 K to cover the range of the stars, and 10–20 Gyr to allow (generously!) for a possible age

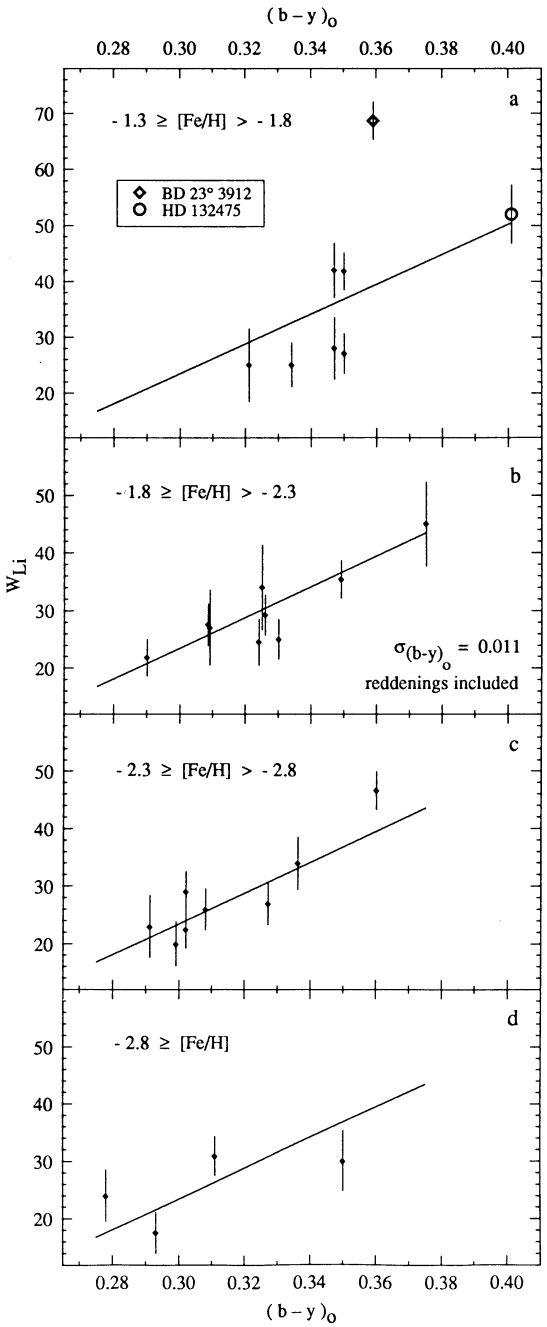

FIG. 3.—Lithium equivalent width vs. $(b-y)_0$ color, binned by metallicity. The solid line is the fit for all stars, from Table 4J, which includes reddening (§ 3.2) and assumes a 2 mÅ minimum uncertainty (§ 2.1.1), and excludes HD 132475 and BD 23°3912 (§ 3.2). No strong systematic effects with metallicity are apparent. (*a*): $1.3 \geq [Fe/H] > -1.8$; (*b*): $1.8 \geq [Fe/H] > -2.3$; (*c*) $2.3 \geq [Fe/H] > -2.8$; (*d*) $-2.8 \geq [Fe/H]$.

spread among the stars, the entire range in log g for this parameter space is 0.6 dex from Revised Yale Isochrones (Green, Demarque, & King 1987) and 0.5 dex from VandenBerg & Bell isochrones (1985). On any given isochrone, the difference in log g between the two edges of the plateau ranged from 0.3 to 0.5 for Yale and 0.2 to 0.4 for VB. However, *at a given color*, a conservative upper limit to the uncertainty in log g seems to be ± 0.1 dex, except possibly near the hot edge of the plateau. Even if we allow variations in log g as large as 0.2 dex, the effect on $b-y$ is less than 0.003, which is small compared to our assumed σ_{b-y} of 0.005, and negligible compared to $\sigma_{(b-y)_0}$ of 0.011 (see § 3.2). Similarly, at fixed color, increasing log g by 0.2 dex increases W_{Li} negligibly (about 1%).

2.4.3. *Chromospheric Activity*

The strengths of some lines are known to vary with chromospheric activity, possibly because of the effects of higher temperature plages and/or lower temperature spots. Boesgaard (1991) has observed some chromospherically active stars, specifically to see whether the strength of the Li line at 6707.8 Å depends on activity. She obtained very high S/N (500–800) on stars with respectably high Li line strengths (her Fig. 4 shows one star with $W_{Li} \sim 41$ mÅ, and another with 104 mÅ), which were monitored through most of a rotation cycle. While rotational modulation of the Ca II K line was observed and also variation of other features, the Li line itself was constant in strength to better than 1% in *all* stars observed, which is quite negligible for the purposes of this paper. By comparison, the much older halo stars are likely to be far less active; in fact, there is only a hint of any activity/spots/magnetic fields in one star, Groombridge 1830 = HD 103095 (Noyes, Weiss, & Vaughan 1984). Therefore, the effects of activity on the Li line in our halo stars are likely to be even more negligible than in the young active stars observed by Boesgaard.

3. χ^2 TESTS IN THE COLOR–W_{Li} PLANE

We separate our analysis in two sections. In § 3.1 we present our method and draw conclusions ignoring the possible effects of reddening. In § 3.2 we explore the implications that result if reddening is considered.

3.1. *Method: No Reddening*

To determine whether the halo star Li data have an intrinsic dispersion, we have performed a number of χ^2 analyses, which are summarized in Table 4A and individually listed in Tables 4B–4N. We first consider the case of theoretically derived σ_W, assuming a minimum error of 2 mÅ per observation (§ 2.1.1). Figure 2*a* shows the weighted mean W_{Li} for each halo star as a function of $(b-y)$, where the W_{Li} and $(b-y)$ are taken from Table 1, including BD 23°3912. The fitting function chosen for the χ^2 analysis is a line of the form $y = Ax + B$ (the data show no evidence in either the W_{Li}-color or the Li–T_{eff} plane of deviation from a linear behavior; note that the Li line in halo stars is weak, unblended, and falls on the linear part of the curve of growth.) A weighted least-squares fit to the data then yields the relation $W_{Li} = 388.4(b-y) - 98.4$ mÅ (Table 4A, case 4b; and Table 4B. Table 4A summarizes the parameters describing each fit discussed below and also lists the table for each fit where details are presented.) In the computation for a value of χ^2/ν (reduced chi-squared, where the number of degrees of freedom ν is 2 less than the number of points N), we wished to take into account the uncertainty in $b-y$. This was done by propagating σ_{b-y} into σ_W for each star using the relation above, assuming $\sigma_{b-y} = 0.005$ mag; i.e., an amount $A\sigma_{b-y}$ (= 1.9 mÅ in this case) was added in quadrature to σ_W for each star, yielding an overall uncertainty σ_W(tot) for each star (the vertical bars in Fig. 2*b* include this contribution).[10]

[10] Strictly speaking, including σ_{b-y} in the total uncertainty affects the determination of the slope and intercept, and thus could in principle alter the confidence limits derived below. To test this, in some cases we iterated by using the new σ_W(tot) to rederive the slope and intercept and the resulting χ^2/ν; we found nearly identical confidence limits as when this iteration was ignored. We thus believe that calculating σ_W(tot) as described above, without iteration, is sufficiently accurate for our purposes.

TABLE 4A

PARAMETERS FOR χ^2 FITS DESCRIBED IN TABLES 4B–4N

Table Number (1)	Reddenings Included? (2)	Uncertainty for W_{Li}: Theoretical (th), or Empirical (emp)? (3)	Stars Excluded from Fit (4)	A (5)	B (6)	Number of Stars (7)	"avg" W_{Li} (8)
4B	no	th (2 mÅ min)	...	388.4	−98.4	29	31.4
4C	no	th (2 mÅ min)	BD 23°3912	294.8	−68.6	28	30.0
4D	no	th (2 mÅ min)	BD 23°3912 and G4−37	324.1	−77.8	27	30.4
4E	no	emp (2.8 mÅ all)	...	339.3	−82.4	29	31.6
4F	no	emp (2.1 & 3.7 mÅ)	...	367.8	−91.8	29	31.6
4G	no	emp (2.8 mÅ all)	BD 23°3912 and G4−37	322.7	−76.9	27	30.6
4H	no	emp (2.1 & 3.7 mÅ)	BD 23°3912 and G4−37	332.5	−80.4	27	30.6
4I	yes	th (2 mÅ min)	HD 132475	354.6	−83.4	28	30.6
4J	yes	th (2 mÅ min)	HD 132475 and BD 23°3912	267.5	−56.8	27	29.2
4K	yes	emp (2.8 mÅ all)	HD 132475	291.5	−63.3	28	30.8
4L	yes	emp (2.1 & 3.7 mÅ)	HD 132475	313.3	−70.7	28	30.9
4M.....	yes	emp (2.8 mÅ all)	HD 132475 and BD 23°3912	250.9	−51.0	27	29.4
4N	yes	emp (2.1 & 3.7 mÅ)	HD 132475 and BD 23°3912	265.7	−55.9	27	29.4

NOTE.—Each line in the table presents parameters for the weighted least-squares fit of a line in the $[(b-y)$ color, lithium equivalent width (in mÅ)] plane for the extreme halo dwarfs listed in Table 1 that have a color determined by SN1. Col. (2) indicates whether the reddenings of SN3 have been considered in the fit, i.e., whether the abscissa is $(b-y)$ or $(b-y)_0$. Col. (3) indicates the minimum uncertainty assumed for the equivalent width of any single measurement. Col. (4) indicates fits that do not use the full sample. Cols. (5), (6), and (7) show the derived slope A, intercept B, and the number of stars used in the fit. Col. (8) shows the average equivalent width as weighted by σ(tot), and thus the effects of col. (3). For each fit, a χ^2 analysis has been performed using several values for the assumed uncertainty in the abscissa. Col. (1) indicates the table describing the results of the χ^2 analysis for each fit.

TABLE 4B

χ^2 ANALYSIS WITH NO REDDENINGS, INDIVIDUAL UNCERTAINTIES, AND 2 mÅ MINIMUM UNCERTAINTY PER MEASUREMENT

Assumed $\sigma_{(b-y)}$ (1)	χ^2 (2)	χ^2/ν (3)	P (4)	σ (5)	W (6)	a (7)	d (8)	Fractional Dispersion (9)
0.003.....	251	9.30	ϵ^2	$\gg 7$	7.5	3.3	6.7	0.21
0.005.....	*173*	*6.40*	ϵ	*>7*	*7.6*	*3.7*	*6.6*	*0.21*
0.010.....	73.3	2.72	3.7×10^{-6}	4.5	7.6	5.1	5.7	0.18
0.013.....	48.6	1.80	6.5×10^{-3}	2.5	7.6	6.0	4.6	0.15
0.014.....	43.0	1.59	2.6×10^{-2}	1.9	7.6	6.1	4.1	0.13

NOTE.—Each of Tables 4B–4I describes the results of a χ^2 analysis for a particular least-squares fit (see Table 4A for the parameters of the fit). Col. (1) gives the assumed total 1 σ uncertainty in the color; unless noted otherwise, the standard case throughout (indicated by italics in the tables) is $\sigma_{b-y} = 0.005$ and $\sigma_{(b-y)_0} = 0.011$. (See text, § 3.1 and § 3.2.) Uncertainties in the equivalent width are combined with col. (1) in the manner described in § 3.1. Cols. (2) and (3) give the resulting value of χ^2 and reduced χ^2. Col. (4) indicates the probability of exceeding the values in the previous two columns. Assuming the fit to be a linear parent function, and assuming an uncertainty as given in col. (1), col. (5) indicates the confidence interval, in terms of number of σ's that the data are *not* distributed randomly about the parent function; i.e., the confidence with which we expect an intrinsic dispersion about the parent function. Cols. (6)–(9) give the width, average uncertainty, dispersion, and fractional dispersion (see text for definitions, § 3.1).

TABLE 4C

χ^2 ANALYSIS WITH NO REDDENINGS, 2 mÅ MINIMUM, EXCLUDING BD 23°3912

Assumed $\sigma_{(b-y)}$ (1)	χ^2 (2)	χ^2/ν (3)	P (4)	σ (5)	W (6)	a (7)	d (8)	Fractional Dispersion (9)
0.003.....	*109*	4.21	3.4×10^{-12}	6.9	4.7	3.2	3.5	0.12
0.005.....	*86.9*	*3.34*	1.7×10^{-8}	*5.5*	*4.9*	*3.5*	*3.5*	*0.12*
0.008.....	58.5	2.29	2.7×10^{-4}	3.5	5.1	4.0	3.2	0.10
0.010.....	46.6	1.79	7.9×10^{-3}	2.5	5.1	4.4	2.7	0.09
0.011.....	41.4	1.59	1.1×10^{-2}	1.98	5.2	4.6	2.3	0.08

TABLE 4D

χ^2 ANALYSIS: NO REDDENINGS, 2 mÅ MINIMUM, EXCLUDING BD 23°3912 AND G4−37

Assumed $\sigma_{(b-y)}$ (1)	χ^2 (2)	χ^2/ν (3)	P (4)	σ (5)	W (6)	a (7)	d (8)	Fractional Dispersion (9)
0.003.....	56.3	2.25	3.3×10^{-4}	3.4	3.5	3.3	1.3	0.04
0.005.....	*42.1*	*1.68*	*1.8×10^{-3}*	*2.9*	*3.6*	*3.5*	*0.6*	*0.02*

TABLE 4E

χ^2 ANALYSIS WITH NO REDDENINGS, AND 2.8 mÅ FOR ALL MEASUREMENTS

Assumed $\sigma_{(b-y)}$ (1)	χ^2 (2)	χ^2/ν (3)	P (4)	σ (5)	W (6)	a (7)	d (8)	Fractional Dispersion (9)
0.003.....	179	6.65	Small	$\geqslant 8$	6.5	3.1	5.7	0.18
0.005.....	*146*	*5.41*	*3×10^{-18}*	*>8*	*6.7*	*3.4*	*5.8*	*0.18*
0.010.....	79.3	2.94	4.8×10^{-7}	4.9	7.2	4.5	5.5	0.18
0.014.....	50.2	1.86	4.2×10^{-3}	2.6	7.3	5.7	4.6	0.14
0.015.....	45.3	1.68	3.1×10^{-2}	1.9	7.3	5.9	4.2	0.13

TABLE 4F

χ^2 ANALYSIS WITH NO REDDENINGS, 2.1 mÅ UNCERTAINTY FOR PRIMARY SAMPLE MEASUREMENTS AND 3.7 mÅ FOR THE OTHERS

Assumed $\sigma_{(b-y)}$ (1)	χ^2 (2)	χ^2/ν (3)	P (4)	σ (5)	W (6)	a (7)	d (8)	Fractional Dispersion (9)
0.003.....	222	8.23	Small	Large	6.5	3.0	5.8	0.18
0.005.....	*162*	*6.02*	*3×10^{-21}*	*>9*	*6.8*	*3.4*	*6.0*	*0.19*
0.010.....	75.6	2.80	1.6×10^{-6}	4.7	7.2	4.7	5.5	0.17
0.014.....	45.8	1.70	1.3×10^{-2}	2.2	7.3	6.0	4.2	0.13
0.015.....	41.0	1.52	4.1×10^{-2}	1.7	7.3	6.3	3.7	0.12

TABLE 4G

χ^2 ANALYSIS: NO REDDENINGS, 2.8 mÅ ALL, EXCLUDING BD 23°3912 AND G4−37

Assumed $\sigma_{(b-y)}$ (1)	χ^2 (2)	χ^2/ν (3)	P (4)	σ (5)	W (6)	a (7)	d (8)	Fractional Dispersion (9)
0.003.....	53.6	2.15	7.5×10^{-4}	3.2	3.6	3.1	1.9	0.06
0.005.....	*42.3*	*1.69*	*1.7×10^{-2}*	*2.1*	*3.7*	*3.4*	*1.5*	*0.05*
0.006.....	37.1	1.49	5.5×10^{-2}	1.6	3.7	3.5	1.1	0.04

TABLE 4H

χ^2 ANALYSIS WITH NO REDDENINGS, 2.1 mÅ FOR PRIMARY AND 3.7 mÅ FOR THE OTHERS, EXCLUDING BD 23°3912 AND G4−37

Assumed $\sigma_{(b-y)}$ (1)	χ^2 (2)	χ^2/ν (3)	P (4)	σ (5)	W (6)	a (7)	d (8)	Fractional Dispersion (9)
0.003.....	76.4	3.06	4×10^{-7}	5.0	3.8	2.9	2.5	0.08
0.005.....	*54.2*	*2.17*	*6.1×10^{-4}*	*3.2*	*3.9*	*3.2*	*2.1*	*0.07*
0.006.....	45.6	1.82	7.1×10^{-3}	2.5	3.9	3.4	1.8	0.06
0.007.....	38.5	1.54	4.1×10^{-2}	1.7	3.9	3.7	1.3	0.04

TABLE 4I

χ^2 ANALYSIS WITH REDDENINGS INCLUDED, 2 mÅ MINIMUM UNCERTAINTY, AND EXCLUDING HD 132475

Assumed $\sigma_{(b-y)_0}$ (1)	χ^2 (2)	χ^2/ν (3)	P (4)	σ (5)	W (6)	a (7)	d (8)	Fractional Dispersion (9)
0.005.....	196	7.52	Small	>7	7.8	3.5	6.9	0.23
0.011.....	*73.6*	*2.83*	*2.0×10^{-6}*	*4.6*	*7.7*	*5.0*	*5.9*	*0.19*
0.014.....	50.3	1.93	2.9×10^{-3}	2.8	7.7	5.9	4.9	0.16
0.016.....	40.2	1.55	3.7×10^{-2}	1.7	7.7	6.6	4.0	0.13

TABLE 4J

χ^2 ANALYSIS: REDDENINGS, 2 mÅ MINIMUM, EXCLUDING HD 132475 AND BD 23°3912

Assumed $\sigma_{(b-y)_0}$ (1)	χ^2 (2)	χ^2/ν (3)	P (4)	σ (5)	W (6)	a (7)	d (8)	Fractional Dispersion (9)
0.005.....	83.2	3.33	3.5×10^{-8}	5.4	4.7	3.4	3.2	0.11
0.011.....	*39.5*	*1.58*	*3.2×10^{-2}*	*1.9*	*4.8*	*4.4*	*2.0*	*0.07*

TABLE 4K

χ^2 ANALYSIS WITH REDDENINGS, 2.8 mÅ ALL, EXCLUDING HD 132475

Assumed $\sigma_{(b-y)_0}$ (1)	χ^2 (2)	χ^2/ν (3)	P (4)	σ (5)	W (6)	a (7)	d (8)	Fractional Dispersion (9)
0.005.....	173	6.66	Small	>7	7.1	3.3	6.3	0.20
0.011.....	*90.1*	*3.46*	*5.4×10^{-9}*	*5.7*	*7.5*	*4.4*	*6.0*	*0.20*
0.018.....	45.2	1.74	1.1×10^{-2}	2.3	7.6	6.1	4.5	0.15
0.019.....	41.5	1.60	2.8×10^{-2}	1.9	7.6	6.3	4.2	0.14

TABLE 4L

χ^2ANALYSIS WITH REDDENINGS, 2.1 mÅ FOR PRIMARY AND 3.7 mÅ FOR THE OTHERS, EXCLUDING HD 132475

Assumed $\sigma_{(b-y)_0}$ (1)	χ^2 (2)	χ^2/ν (3)	P (4)	σ (5)	W (6)	a (7)	d (8)	Fractional Dispersion (9)
0.005.....	238	9.15	Small	>7	7.9	3.2	7.2	0.23
0.011.....	*98.0*	*3.77*	*2.8×10^{-10}*	*6.2*	*8.0*	*4.6*	*6.6*	*0.21*
0.018.....	44.0	1.69	1.5×10^{-2}	2.2	7.9	6.4	4.6	0.15
0.019.....	40.0	1.54	3.9×10^{-2}	1.8	7.9	6.7	4.1	0.13

TABLE 4M

χ^2 ANALYSIS WITH REDDENINGS INCLUDED, 2.8 mÅ UNCERTAINTY FOR ALL STARS, EXCLUDING HD 132475 AND BD 23°3912

Assumed $\sigma_{(b-y)_0}$ (1)	χ^2 (2)	χ^2/ν (3)	P (4)	σ (5)	W (6)	a (7)	d (8)	Fractional Dispersion (9)
0.005.....	89.0	3.56	4.1×10^{-9}	5.8	4.9	3.2	3.8	0.13
0.011.....	*46.8*	*1.87*	*5.1×10^{-3}*	*2.6*	*5.0*	*4.1*	*2.9*	*0.10*
0.012.....	42.2	1.69	1.7×10^{-2}	2.1	5.0	4.3	2.6	0.09
0.013.....	38.2	1.53	4.4×10^{-2}	1.7	5.0	4.4	2.3	0.08

TABLE 4N

χ^2 ANALYSIS WITH REDDENINGS INCLUDED, 2.1 mÅ UNCERTAINTIES FOR PRIMARY SAMPLE AND 3.7 mÅ FOR THE OTHERS, EXCLUDING HD 132475 AND BD 23°3912

Assumed $\sigma_{(b-y)_0}$ (1)	χ^2 (2)	χ^2/ν (3)	P (4)	σ (5)	W (6)	a (7)	d (8)	Fractional Dispersion (9)
0.005.....	121	4.86	Small	>6	5.4	3.1	4.4	0.15
0.011.....	*53.0*	*2.12*	*8.9×10^{-4}*	*3.1*	*5.3*	*4.2*	*3.4*	*0.12*
0.013.....	41.6	1.66	1.9×10^{-2}	2.1	5.3	4.6	2.7	0.09
0.014.....	37.1	1.49	5.6×10^{-2}	1.6	5.3	4.8	2.3	0.08

If we assume that a line is indeed a correct fitting function, then the value of χ^2/ν is a measure of the likelihood that the points are distributed randomly about the fitting line with the uncertainties that are assumed. If the value is much higher than 1, then either the uncertainties are underestimated, or the data exhibit an intrinsic dispersion about the fitting function. The present fit ($N = 29$, $\nu = 27$) yields $\chi^2/\nu = 6.40$ (Table 4B); this has a very small probability of occurring by chance if our uncertainty estimates are accurate (i.e., there is probability $P \ll 10^{-20}$ of obtaining a larger value for χ^2/ν). Column (5) in Tables 4B–4N gives the confidence level in terms of σ at which the value of χ^2/ν implies a dispersion; for the present fit, a dispersion is implied at the greater than 7 σ confidence level. Two points, however, are far more discrepant than the rest: these are BD 23°3912 and G4−37. Both are discussed below, but for the present let us remove them one at a time. Removing BD 23°3912 and repeating the analysis yields χ^2/ν ($N = 28$) = 3.34, $P = 1.7 \times 10^{-8}$ (5.5 σ; Table 4C); removing also G4−37 yields χ^2/ν ($N = 27$) = 1.68, and the probability of obtaining this value by chance is still small, $P = 1.8 \times 10^{-3}$ (2.9 σ; Table 4D). The solid line in Figure 2*b* is the fit obtained from this last case. Note that to bring χ^2/ν down to a value of 1 requires $\sigma_{b-y} = 0.0085$ in the last case and much larger σ_{b-y} in the previous cases.

Similar results are obtained if we consider instead the empirically derived σ_W. When all stars are included, we obtain χ^2/ν ($N = 29$) = 5.41, $P = 3 \times 10^{-18}$ (>8 σ; Table 4E) for the case where a 2.8 mÅ uncertainty is assigned to all measurements, and χ^2/ν ($N = 29$) = 6.02, $P = 3 \times 10^{-21}$ (>9 σ; Table 4F) for the case where 2.1 mÅ uncertainty is assigned to each measurement in the "primary sample" and 3.7 mÅ to the rest. When BD 23°3912 and G4−37 are removed, we obtain χ^2/ν ($N = 27$) = 1.69, $P = 1.7 \times 10^{-2}$ (2.1 σ; Table 4G) for the 2.8 mÅ case, and χ^2/ν ($N = 27$) = 2.17, $P = 6.1 \times 10^{-4}$ (3.2 σ; Table 4H) for the 2.1 and 3.7 mÅ uncertainty case (bringing χ^2/ν down to a value of 1 requires $\sigma_{b-y} = 0.009$ and 0.010, respectively); again the probabilities of obtaining these results by chance remain small.

Therefore, assuming that a line is an appropriate fitting function to the data, and assuming that the uncertainties estimated above are realistic, the values of χ^2/ν strongly suggest that there is indeed some intrinsic dispersion in the halo star lithium abundances. Tables 4B–4N also show results for values of σ_{b-y} other than our assumed 0.005. If the typical uncertainty is in fact smaller than this (§ 2.2, and if the errors discussed in § 2.4 continue to be negligible; and/or if a smaller minimum uncertainty than 2 mÅ is applicable), then the conclusion that a dispersion exists is obtained at still higher confidence levels.

We roughly estimate the magnitude d of the average intrinsic dispersion by assuming that it combines in quadrature with the errors to give the observed total dispersion: first, we define the average uncertainty, a, as the sum of all the σ_W(tot) (which includes errors both in the equivalent widths and in the colors) divided by the number of stars N. We then arbitrarily define a "width,"

$$w = \frac{\chi^2}{\sum_i}\left(\frac{1}{\sigma_i^2}\right),$$

which we suppose to be analogous to the standard deviation of the fit in the case where all the weights are equal. Then, $d = (w^2 - a^2)^{1/2}$. Using the average $W_{\rm Li}$ of about 30 mÅ, a fractional dispersion of order ±10% around the mean is obtained (or equivalently, ±20% [2 σ range]). These quantities are given in columns (6)–(9) of Tables 4B–4N.

The interesting star, BD 23°3912, has been included in the analysis on account of its high Li abundance, even though this star misses the conservative velocity cutoff for extreme stars ($V_{\rm LSR}$ = 125 or 126 km s^{-1} according to the sources quoted in DDK). A possible danger is the (perhaps small) possibility that slightly nonextreme objects formed out of material already enriched in Galactic Li. Nevertheless, the abundance determinations of this star (SS2, RMB) are low, [Fe/H] = −1.6 and −1.3, and it is possible that this star is a genuine halo star approaching the apex of its trajectory. BD 23°3912 has $W_{\rm Li} = 70 \pm 2$ mÅ at a color where the mean is $W_{\rm Li} = 43$ mÅ, assuming the fit from either Table 4C, 4G, or 4H, or 39 mÅ if reddening is considered (§ 3.2) and the fit of any of Table 4J, 4M, or 4N is employed. This is almost a factor of 2 above the mean. This star could perhaps fit attractively as an underdepleted candidate in a scenario where rotationally induced mixing has caused significant depletion (PDD).

The one star, G4−37, which appears to fall clearly below the mean trend (Fig. 2*a*) by about a factor of 2 in abundance is one of the stars which appear to have rather significant reddening.

3.2. *With Reddening*

The example of G4−37 illustrates clearly that individual reddenings must be considered carefully before deriving lithium abundances in the more distant halo stars. This is emphasized by the work of HT, who used the strength of the interstellar Na I absorption to estimate reddenings toward their stars and found that reddening can be very patchy. In particular, HT found that the reddening toward G4−37 is unexpectedly strong, especially since the more distant star ξ Ari, which is only 7° away in the sky, shows almost no reddening. Unfortunately, at present such detailed and direct information on individual stars is quite limited. We do have available, however, the photometric reddenings of SN3.

SN2 have used nearby unreddened stars to derive an intrinsic color relation between the $(b - y)$ index, which is affected by interstellar reddening, and the β index, which is free from interstellar reddening effects. This calibration was then used to obtain the reddening $E(b - y)$ from direct observations of more distant stars (given in SN3, and listed in col. [6] of Table 1).[11] SN3 state $\sigma_{E(b-y)} \sim 0.01$, which we have adopted.[12] We have added this in quadrature to σ_{b-y} to obtain $\sigma_{(b-y)_0} = 0.011$. Evidently, the uncertainty in the reddening by far dominates the uncertainty in the dereddened color. On average, this is too large an uncertainty since most stars in our sample are in

[11] It should be noted that Laird, Carney, & Latham (1988) have also derived reddenings for halo stars from their sample, using the maps of Burstein & Heiles (1982) and of Paresce (1984) and an assumption of smooth dust distribution along the line of sight. They derive a reddening for G4−37 of $E(B-V) = 0.05$. Although the maps do show patchiness, as the example of G4−37 and ξ Ari shows, it is probable that they are not sufficiently detailed for the precision demanded by the present work. We use the reddenings of SN3 instead because they are directly calculated for each star. Note that SN2 and Laird et al. agree in that most nearby halo stars have near-zero reddening (though note that Laird et al. *assume* zero reddening for stars closer than 50 pc), but there is a poor correlation between the two studies for stars that are somewhat reddened (SN2).

[12] SN2 have plotted a histogram of their reddenings for their sample and find that for stars within 100 pc there is a symmetric distribution about $E(b - y) = 0.000$ with standard error of about 0.010 mag, and with a slight tail toward positive values of E. Including stars that are further away increases the relative size of the tail.

fact nearby. The most accurate treatment of colors is in fact to attempt to deredden only the most distant, significantly reddened stars. Nevertheless, we prefer to err on the side of caution, and adopt an uncertainty $\sigma_{(b-y)_0} = 0.011$ for all stars.

When W_{Li} is plotted against the dereddened $(b-y)_0$ in Figure 2*d*, some interesting changes become manifest. First, the whole sample appears shifted to the blue as a group (e.g., compare Figs. 2*a* and 2*c*, or Figs. 2*b* and 2*d*). Second, G4−37 has shifted significantly and has in fact marginally joined the plateau; we adopt SN's relatively high reddening for this star of $E(b-y) = 0.064$ (see also footnote 12). Finally, there are two stars, HD 160617 and HD 132475, with $(b-y)_0$ such that they appear to be above the plateau. Note that for neither star did SN measure the beta index themselves (but they have done so for all other stars in our sample). We *have not plotted* these stars in the dereddened positions for the following reasons.

HD 160617.—In its dereddened position near the hot edge of the plateau, HD 160617 has $W_{Li} = 42 \pm 4$ mÅ at a color $[(b-y)_0 = 0.288]$ where the fit to the data (Table 4A, case 4J) yields $W_{Li} = 20$ mÅ, i.e., a factor of 2 above the plateau. However, P. E. Nissen (1991, private communication) has recently done a detailed analysis of this star using high-resolution ESO CASPEC spectra, and derives $T_{eff} = 5800$ K [consistent with $(b-y)_0 = b-y = 0.347$] by requiring that the iron abundance derived from individual Fe I lines must be independent of excitation potential of the line. [Note that in this manner, Nissen can confirm also the reddening of $E(b-y) = 0.064$ for G4−37.] Indeed, for this star SN borrowed the beta index from Hauck & Mermilliod (1985). This heterogeneous catalog is less accurate and much less uniform than the measurements of SN. We conclude that the beta measurement is likely to be in error, and ignore it, and adopt (possibly conservatively) a reddening of zero. [Figs. 2*c*, *d* show this star plotted with $E(b-y) = 0$]. Note that even with zero reddening, this is one of the most discrepant stars in the sample, above the mean trend. Thus, *any* amount of reddening would strengthen the case for dispersion. The uncertainties in Nissen's work will tolerate an $E(b-y)$ of up to ~ 0.015 for this star. (See also Perrin 1986, and Bessell & Norris 1982 for slightly higher T_{eff} estimates, and a slightly lower $b-y$ measurement.) Finally, we point out the peculiarity that this star is nitrogen-rich (Bessell & Norris 1982), so it is not inconceivable that the material out of which HD 160617 formed may have been already enriched in Galactic Li (e.g., see § 7.2.5 in Deliyannis 1990); however, the equally nitrogen-rich (and approximately similar-[Fe/H]) HD 74000 *does not* appear above the mean trend (Fig. 2).

HD 132475.—In its dereddened position, this star has $W_{Li} = 52 \pm 4$ mÅ at a color $[(b-y)_0 = 0.355]$ where the fit (Table 4A, case 4J) yields $W_{Li} = 38$ mÅ, i.e., approximately a 40% higher abundance than the mean. In this case SN borrowed the beta index from the catalog of Olsen (1983), and because SN1 took great care to be on the same standard photometric as Olsen, the beta index is probably correct. However, SN3 note this star as an RV-variable, which may mean it is a binary, which sometimes introduces a spurious reddening. [Note, however, that using artificial binaries, SN2, conclude that, for the stars similar to the ones considered here, binarity induces an $E(b-y)$ of less than 0.01, usually much less.] Furthermore, this star is nearby. Laird et al. estimate a distance of only 30 pc, and DDK estimate 37 pc based on a parallax of 0.0273 ± 0.0055; in either case significant reddening is unexpected. HD 132475 has *U*, *B*, *V*, *R*, *I*, *J*, *H*, *K* colors available (Carney 1983; Laird et al.), and it has been the object of fine analyses by Hearnshaw (1976) and by Foy & Proust (1980). The $V-K$ and $R-I$ colors are in good agreement with the observed $b-y$, all corresponding to $T_{eff} \sim 5500$ K, using the temperature calibrations given in HD. If the star is dereddened by the amount indicated by the beta index, all color indices indicate a $T_{eff} \sim 5800$ K. The latter temperature is in good agreement with those of the fine analyses; the former are not, supporting the suggested reddening. However, dereddening in a $J-K$, $V-K$ diagram (the most sensitive of the broad-band colors, Carney 1983) causes the star to be discrepant. Whether HD 132475 is reddened is thus uncertain. To be conservative, we drop it from consideration.

If we apply the χ^2 analysis to the dereddened colors, assume the theoretically derived errors with a 2 mÅ minimum, and include BD 23°3912, we find χ^2/ν $(N = 28) = 2.83$, and the probability of obtaining this by chance is still small, $P = 2.0 \times 10^{-6}$ (4.6 σ; Table 4I). Removing BD 23°3912 yields χ^2/ν $(N = 27) = 1.58$, $P = 3.2 \times 10^{-2}$ (1.9 σ; Table 4J). The solid line in Figure 2*b* is the fit obtained from this last case. Including BD 23°3912, and assuming the empirically derived error of 2.8 mÅ per measurement yields χ^2/ν $(N = 28) = 3.46$, $P = 5.4 \times 10^{-9}$ (5.7 σ; Table 4K), while assuming 2.1 mÅ for the "primary sample" and 3.7 mÅ for the rest yields χ^2/ν $(N = 28) = 3.77$, $P = 2.8 \times 10^{-10}$ (6.2 σ; Table 4L). Removing BD 23°3912, and assuming 2.8 mÅ for all yields χ^2/ν $(N = 27) = 1.87$, $P = 5.1 \times 10^{-3}$ (2.6 σ; Table 4M), whereas assuming 2.1 mÅ and 3.7 mÅ yields χ^2/ν $(N = 27) = 2.12$, $P = 8.9 \times 10^{-4}$ (3.1 σ; Table 4N). Once again, the magnitude of the dispersion is of order $\pm 20\%$ (2 σ range). We emphasize that this is only a rough estimate, and also that in specific cases the dispersion may be larger. For example, consider the six stars with $(b-y)_0 \sim 0.350$ (Fig. 2*d*). Assuming the fit from case 4M (Tables 4A and 4M), and computing χ^2/ν implies a dispersion of $\pm 30\%$ (2 σ range; at greater than 3 σ confidence levels, even though the sample is quite small); removing the star that falls right on the fit now implies a dispersion of $\pm 36\%$ (2 σ range; at even higher confidence levels). Considering the same six (or five) stars without reddenings, and assuming the fit from case 4G yields very similar results, $\pm 30\%$ (or $\pm 34\%$; 2 σ ranges), but at still higher confidence levels.

With or without reddening, and with or without BD 23°3912, the evidence for a real dispersion remains strong.

4. DISCUSSION

We have found that taking the uncertainties at face value, regardless of whether they are determined theoretically or empirically, implies that there is dispersion in the halo star lithium equivalent widths at fixed color. According to current understanding of model atmospheres, and also to observational evidence (such as that the Li line does not appear to vary in time in well-studied chromospherically active stars), this implies an intrinsic dispersion in the Li abundances themselves. Even when uncertainties that seem unrealistically large are considered, this result remains near or above the 2 σ confidence level. The magnitude of the dispersion seems to be rather small on average, on the order of $\pm 20\%$ (2 σ range) in abundance, but could be higher in specific cases. We emphasize that this is only a rough estimate of the dispersion. However, there is the hope that numerous new observations would further test these conclusions and yield improved estimates for the magnitude of the dispersion.

What, then, might be the origin of this dispersion? We examine various possibilities below.

4.1. *Standard Stellar Models*

Consider first the possibility that all Group A stars formed with the same Li abundance, and that there was no prior Galactic Li enrichment nor any subsequent stellar destruction. The expected observed abundances would form a completely flat plateau in the Li-$T_{\rm eff}$ plane, and would be equal to $\rm Li_p$. For $T_{\rm eff} \geq 5000$ K and [Li] ~ 2, this plateau is represented approximately by a line in the W(Li)–color plane, with positive slope (e.g., see the two lines of constant abundance in Fig. 4). No dispersion would be expected in either plane, beyond measurement errors and unforeseen differences in the stellar atmospheres. In contrast to these expectations, dwarfs cooler than 5500 K are known to exhibit depleted Li abundances relative to the hotter stars. In fact, it has been argued that (in the Li–$T_{\rm eff}$ plane) the plateau itself has a slight slope, still linear in both planes, with decreasing abundance for decreasing $T_{\rm eff}$ (RMB; Deliyannis & Demarque 1991a, hereafter DD). This is confirmed in the W(Li)–color plane, where fits to the data have shallower slope than lines of constant abundance (Fig. 4).

Thus, it is necessary to take into account effects that can cause deviation from a constant abundance, and in particular stellar evolution effects (it is unlikely that Galactic enrichment from some lower abundance can, by itself, conspire to produce the patterns described above). DDK showed that standard stellar evolutionary models can reproduce the Li depletion dependence on $T_{\rm eff}$, both in the plateau and cool stars (as well as in subgiants) by burning Li at the base of the surface convection zone (or diluting). (The DDK models develop a steeper slope near the cool portion of the plateau, consistent with the data, but because of the paucity of data in that region, a straight line through the plateau stars fits just as well, in both planes.) Is a dispersion consistent with the predictions of DDK? Assuming a constant mixing length, dispersion at a given $T_{\rm eff}$ may be introduced in two ways: as a result of the range in stellar metallicities, and as a result of the possibility of an age spread (e.g., $\sim$2 Gyr). Not only do models with the same mass but different metallicity deplete Li differently, but they also have different $T_{\rm eff}$ at a given age; furthermore, the models evolve to hotter $T_{\rm eff}$ with age (see DDK and DD for details). Figure 5 shows a magnification of standard Li isochrones from the models of DDK for $Z = 10^{-4}$ and $Z = 10^{-3}$ (i.e., [Fe/H] = -2.3 and -1.3), $Y = 0.24$, for 15 and 17 Gyr, where the same models imply an age of $\sim$16 Gyr for the oldest globular clusters. Excluding HD 132475 and BD 23°3912, all but two stars have $(b-y)_0 > 0.355$ (Fig. 2*b*), i.e., $T_{\rm eff} > 5835$ K according to equation (2). At 5800 K, the combined effects of a metallicity range and an age spread result in an abundance spread of 0.03 dex, or a dispersion of $\pm 3.5\%$ (Fig. 5). The dispersion becomes even smaller for higher $T_{\rm eff}$ and is less than $\pm 1.5\%$ for $T_{\rm eff} \geq 6200$ K. (These numbers are made slightly larger if one extends all the way to $Z = 10^{-5}$; however, analysis of the data suggests [see also Fig. 4] that the same dispersion of roughly $\pm 10\%$ [or $\pm 20\%$ 2 σ range] is exhibited in each of the metallicity bins.) The dispersion is also smaller if the age range is centered around an age smaller than 16 Gyr. Although we consider our estimate of $\sim \pm 20\%$ (2 σ range) for the observed dispersion to be quite rough, it nonetheless seems to exceed the dispersion expected from standard models alone. This conclusion could be tested further by new observations concentrated near the hot edge of the plateau. For $T_{\rm eff} < 5800$, the predicted dispersion increases, but the current paucity of observed stars precludes a meaningful comparison.[13] It is worth noting the possibility that isochrones of different metallicity may show less dispersion when models with updated opacities are produced.

It thus seems necessary to search for alternate sources of dispersion. One possible source might be differentially localized Galactic Li enrichment occurring in the very early stages of Galactic evolution. It cannot be ruled out that such a source together with standard models might account for the observations. However, to be viable, the Galactic Li enrichment scenario must pass certain observational constraints (see § 4.3 below).

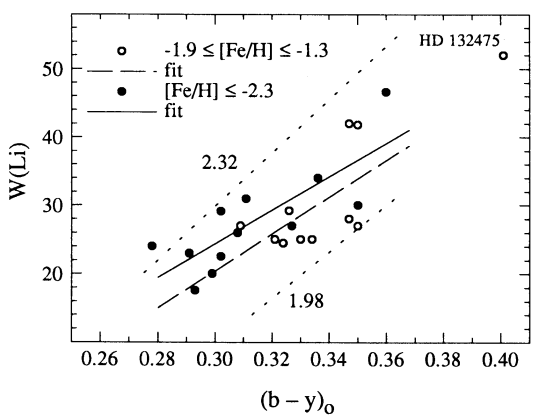

FIG. 4.—Metal-poor (*filled circles*) and metal-rich (*open circles*) subsets, with simple fits to each subset, excluding BD 23°3912 and HD 132475. Approximate lines (*dotted*) of constant abundance (as indicated) are also shown, derived from Fig. 6 of HD, assuming [Fe/H] = -2 and log $g = 4.5$.

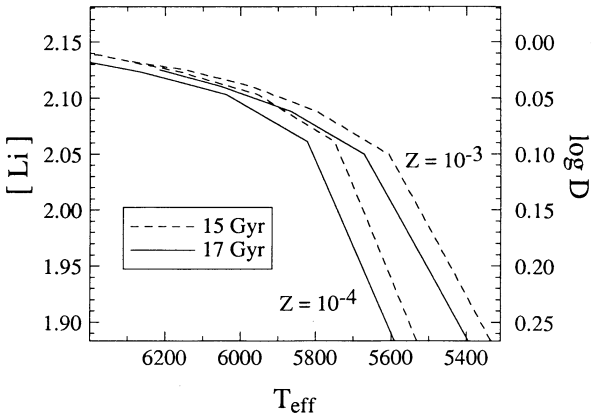

FIG. 5.—Magnification of standard stellar Li depletion isochrones from DDK. The two on the (left, right) correspond to $Z = 10^{-(4,3)}$.

[13] Note that there exists one star with $T_{\rm eff}$ between 5500 and 5800 K, namely G238 – 30, that may have the lowest yet detected plateau abundance (DD). Unfortunately, SN did not obtain Strömgren photometry for this star (and it has been excluded from our analysis), but if we use equation (2) to convert its $T_{\rm eff} = 5600 \pm 100$ K to $(b-y)_0 = 0.388 \pm 0.014$, and use W(Li) = 33 ± 6 mÅ from Spite et al. 1987 (SSPC), then it does indeed seem possible that this star might be located below the mean trend (Fig. 2*d*, where the total vertical error bar includes contributions from $\sigma_{(b-y)}$, σ_E, and σ_W.) Note also that "reconverting" from $T_{\rm eff}$ to color indeed results in a far larger error than the purely relative $\sigma_{(b-y)}$.

4.2. *Rotational Stellar Models*

Another possibility is that rotationally induced mixing has depleted the Li abundances from a significantly higher Li_p, and in so doing has introduced some dispersion (PDD). It must be emphasized that standard stellar models neglect a number of additional physical mechanisms that could be acting in stars to alter the surface Li abundance. In fact, standard models cannot explain many of the observed features of Li and Be depletion in Population I stars (including the Sun, see, e.g., Sofia, Pinsonneault, & Deliyannis 1991). It is only reasonable to suppose that whatever mechanisms are responsible for producing these features in Population I stars might also have been important in the much older halo stars. In fact, Population I analogs of the PDD models can explain these features. It is thus worth outlining briefly the assumptions behind the models of PDD, pointing out some of the explained features in Population I stars, and to discuss their prediction that a small Li dispersion might exist in the halo stars.

The rotational models of PDD are based on the approach of Endal & Sofia (1976, 1978, 1981). This method has been recently improved and applied to the Sun (Pinsonneault et al. 1989) and to Population I clusters (Pinsonneault et al. 1990), and utilizes a large body of observational data. The models begin evolution in the early, fully convective pre–main-sequence, and are assigned an initial angular momentum (J_0). The magnitudes and distribution in J_0 are chosen to agree with T Tauri data and with appropriate extrapolations (Kawaler 1987) of the Kraft (1967) curve. The models are then forced to lose angular momentum from the surface to match the observed spin-down of stars (e.g., Skumanich law 1972), in agreement also with a simple magnetic wind model (Kawaler 1988). Throughout the interior, a number of both secular and dynamical instabilities are modeled (including meridional circulation). Angular momentum is conserved locally until an instability occurs, at which point angular momentum is transferred to relieve the instability. A small amount of mixing is associated with the transport of angular momentum and is calibrated to match the solar lithium depletion. It is worth noting that this calibration automatically gives a beryllium depletion that is consistent with the difference between the meteoritic and photospheric abundances; it also reproduces the morphology of the lithium abundances both within a cluster (i.e., as a function of mass) and in clusters of different ages (i.e., as a function of time), and naturally creates a J_0-dependent dispersion in the lithium abundance at fixed $T_{\rm eff}$, as is observed. This includes reproducing the Boesgaard Li gap in F stars. Furthermore, Population I rotational models pass another serious constraint: they quantitatively reproduce the simultaneous (and finite) depletion of *both* lithium and beryllium observed in some stars (Deliyannis & Pinsonneault 1992). There are also hints that this type of modeling may explain the CNO abundance changes observed on the giant branches of open *and globular clusters* (Pinsonneault et al. 1991). For a recent review of these and other applications, see Sofia et al. (1991).

The models of PDD are an application of this approach to Population II stars. The models reproduce the morphology of the halo lithium observations (which is very different from that of Population I stars), both the plateau and the (further) depleted cool dwarfs, and do so while depleting the lithium abundance by about an order of magnitude. The profound implications of this result for cosmology necessitate as thorough a testing of the models as possible. One test that is especially relevant here is the prediction of a J_0-dependent dispersion in the lithium abundances. This is *in addition* to the dispersion introduced as a result of ranges in metallicity and age (§ 4.1). The magnitude of the dispersion induced by ranges in Fe and age is approximately the same in rotational models as in standard models. As in the Population I case, the PDD models predict a J_0-dependent dispersion but, for reasons that are well understood and related to the differences in structure between Population I and Population II models, the magnitude of the dispersion is smaller in the Population II case, being less than a factor of 2 for a range of a factor of 10 in J_0 for J_0 that bracket the distribution in J_0 observed in Population I stars of comparable mass. As there are no young Population II objects around, the Population II distribution in J_0 is not known directly. However, one might assume that it is highly peaked, as seems to be the case for Population I stars of similar mass, with a range for most such stars of less than a factor of 3. For such a range centered around $\log J_0 = 49.7$ (case J1 of PDD, see Fig. 6 therein) the models predict only a small dispersion in Li of about 0.1 dex, or $\pm 13\%$. This is consistent with the results of this paper.

So in contrast to standard models, which require some early Galactic Li production mechanism to explain the dispersion at all relevant $T_{\rm eff}$, the rotational models can, by themselves, account for this dispersion. Of course, this does not argue against early Li production mechanisms; it merely eliminates their *necessity* to explain the data. In fact, since the rotational models predict an initial abundance of order 3.1, such early production mechanisms would be consistent with the rotational scenario even if they produce a significantly larger abundance of Li than ~ 2. Such production mechanisms would only run afoul of the observations (in the rotational scenario) if they produced a large dispersion in the initial Li abundances at a level of ~ 3.1.

Finally, we speculate on some marginal points of consistency. First, slightly more dispersion is observed in slightly more metal-rich stars than our Group A sample, e.g., for $-1.3 > [Fe/H] \geq -0.9$, and even more for $-0.9 > [Fe/H] \geq -0.6$ (e.g., Deliyannis 1990). This pattern is reproduced by rotational models (unpublished) we have computed for the relevant metallicities, again with initial abundances above 3. Second, if we bin the data into just two groups, a metal-poor one with $[Fe/H] \leq -2.3$, and a metal-rich one with $-1.9 \leq [Fe/H] \leq -1.3$ (excluding again HD 132475 and BD 23°3912), we find that a fit to the metal-rich group falls slightly *below* that for the metal-poor group (Fig. 4). If this effect is real, it might argue *against* Li enrichment from the metal-poor group to the metal-rich group (in the context of depletion from standard stellar models and low Li_p). Furthermore, close examination of Figure 6 in PDD shows that just such an effect with about the same magnitude is predicted by the rotational models of PDD in the plateau region, assuming the same (high) initial Li for both metallicity groups. Third, there is the expectation that occasionally (but rarely), a star may have formed with very low J_0 and should thus have a measurably higher lithium abundance according to PDD. BD 23°3912 might in fact be such a case. While these points of consistency may be provocative, they do not currently provide strong evidence in favor of rotational mixing. More thorough testing of the PDD models, and the prospect of discovering additional stars like BD 23°3912 will require numerous new observations. The models of PDD can perhaps also be tested with observations

of stars that have not spun down in the manner that normal stars do. It is possible, for example, that tidally locked binaries of sufficiently short period may have spun down during the fully convective pre–main-sequence, and they may thus have avoided lithium depletion due to rotationally induced mixing (DDK, PDD). This effect has possibly already been observed in the Hyades (Soderblom et al. 1990) and in the intermediate metallicity star BD $-0°4234$ (Deliyannis 1990).

4.3. *Galactic* Li *Enrichment*

We now return to the possibility that Galactic Li enrichment could instead be causing the dispersion. Many Li production mechanisms have been proposed (for reviews, see, e.g., Boesgaard & Steigman 1985; Deliyannis 1990). Though it is difficult to assess most of them quantitatively, viable Li enrichment mechanisms for the *early* Galaxy must pass certain constraints. According to the presently available data, they must be independent of metallicity for [Fe/H] ≤ -1.3 (§ 2.4.1, Fig. 3). Furthermore, since the hottest halo stars are also the most metal poor (and perhaps also the very oldest), a dispersion in those stars would require Galactic Li enrichment to have occurred on a short time scale. This would be particularly true if future observations show that evidence for dispersion persists even in turnoff stars with [Fe/H] < -3.

We can comment on one mechanism, spallation induced by cosmic rays, that has received attention recently, and that probably accounts for the Galactic evolution of Be and perhaps also much of the B. The Be abundance in metal-poor stars rose sharply with metallicity (Ryan et al. 1990; Ryan et al. 1992, hereafter RNBD), while the Li abundance apparently remained approximately constant. Recently, the cosmic-ray models of Steigman & Walker (1992; SW) have suggested that if cosmic rays produced the observed Be, then they could have also produced a nontrivial fraction of the Li observed in halo stars. It should be emphasized that *this assumes that* [Li_p] *is not much larger than* 2.0*; if, on the other hand* [Li_p] $\gg 2$ (*as, e.g., inferred from the rotational models of PDD*), *then the* Li *produced by the cosmic-ray models of SW would be negligible.* Inspection of the observed Be and Li reveals a possible inconsistency, which can be resolved if [Li_p] $\gg 2$. The inconsistency comes about because the high-metallicity (halo) star HD 76932 has high Be but low Li, whereas the low-metallicity star HD 84937 has higher Li and a very low upper limit to Be. In more detail: Table 5 lists the halo stars observed for Be by RNBD. If the observed Be was produced by Galactic cosmic rays (GCR), the corresponding predicted amount of $^7Li_{GCR}$ is given in column (5) (using eqs. [7] and [8] of SW)[14]. The resulting $^7Li_{GCR}$ appear to be increased discernibly with metallicity; a significant $^7Li_{GCR}$ contribution to the observed Li abundances (with [Li_p] ~ 2) thus appears to be in conflict with the data (Fig. 3). We emphasize that this comes out of the prediction of SW for the $^9Be/^7Li$ ratio, combined with the highest quality Be observations available at present (though still only few in number). Consider next HD 84937, which is predicted to have the smallest $^7Li_{GCR}$. Subtracting this from $^7Li_{obs}$, we can assume that what is left is Li_p (derived best for this star since its $^7Li_{GCR}$ contribution is predicted to be small); thus [Li_p] > 2.07 (col. [7]). This assumption is not foolproof, since other sources (or even cosmic rays, conceivably) could have already produced more Li without having produced Be. If we now demand (as did RNBD) that all halo stars must have formed with an amount of ^7Li at least as great as Li_p, then HD 76932 is predicted to have more total [^7Li] (>2.37) than is observed (1.96).[15] Assuming that the SW models are correct, this suggests that the ^7Li in HD 76932 has been depleted. But how? *HD 76932 is a subgiant* (not cool enough for dilution to have begum, as evidenced, e.g., by the cooler HD 140283), which implies that its main-sequence turnoff was near the hot edge of the plateau (about 6100 K for its metallicity, or hotter if this star is younger than average), where standard models are best at preserving ^7Li (less than 0.04 dex depletion). The discrepancy disappears if [Li_p] is in fact much larger than 2.0 (so that the contribution of Li_{GCR} to Li_p is negligible), and depletion has occurred by rotational mixing, which can also overdeplete this star slightly relative to other stars. But we must caution again that the uncertainties in the predictions of the SW models may be nontrivial. Clearly, it is important to test these arguments further by additional observations of Be and ^6Li (and B) in metal-poor stars.

Finally, a comment on Galactic Li enrichment: two possible scenarios are often discussed (indeed, hotly debated!) regarding the evolution of the Galactic Li abundance. One scenario has the Galactic Li abundance apparently increasing by about an order of magnitude from the observed Population II (and consistent with the standard halo star models of DDK) to the observed Population I (see, e.g., Boesgaard & Steigman 1985; Mathews, Alcock, & Fuller 1990). The other assumes that the Population I abundance (often quoted as being ~ 3.0) is primordial and that destruction of Li has taken place in the Population II stars. According to the rotational models of PDD, *a third possibility* emerges: that $Li_p \sim 3.1$, that the local Li abundance of 4.5 Gyr ago was enriched to 3.3 (from meteoritic data), and that the current abundance may be even higher (from fitting of the rotational models to open cluster data, but also from *direct observations* in T Tauri stars and other pre–main-sequence stars).

5. CONCLUSION

We have presented evidence that there exists a small dispersion in the lithium abundances of extreme halo dwarfs. This dispersion cannot be accounted for by standard stellar models

[14] ^6Li is ignored since it is mostly destroyed (DDK; Deliyannis 1990) and anyway observed to have a low upper limit in these two stars [Maurice, Spite, & Spite 1984; PHD], while the predicted ratio is $^6Li_{GCR}/^7Li_{GCR} \sim 1$.

[15] Let us push several of the uncertainties all in the same direction to try to minimize this discrepancy; i.e., let us accept a higher [Fe/H] for HD 76932 and a lower [Fe/H] for HD 84937 (-1.0 and -2.4), the lower Be abundance for HD 76932 of RNBD (0.70), and lower Li_{obs} for HD 84937 (2.10); we then derive a total ^7Li abundance for HD 76932 of 2.21, which is still marginally high compared to the observed 1.96. We stress that to make the abundances match better would require that the errors are even larger than assumed in this example, and that they combine in the right way. If, conversely, we push the uncertainties the other way, using [Fe/H] $= (-1.3, -2.0)$, Be of 0.85 and Li_{obs} of 2.2, then the total derived ^7Li abundance for HD 76932 is 2.53, which is very discrepant from the observed 1.96. Note that HD 76932 is slightly too metal-rich to be included in the Group A extreme sample, and recall that the sample was purposely chosen to be extreme in part to minimize candidates that may have already been enriched in Galactic Li. However, if the material that formed HD 76932 had been Li-enriched from *any* source, then the discrepancy is further exacerbated.

New, and higher quality, observations made recently at CFHT suggest that the Be abundance in HD 76932 may be even slightly higher than 0.85, and an apparent detection in HD 84937 is at or just slightly below the upper limit of RNBD (A. M. Boesgaard, 1992, private communication); this too exacerbates the discrepancy. These observations suggest that the uncertainty in the Be abundance of HD 76932 is of order 0.1 dex, and maybe slightly higher in HD 84937; for the other two stars in Table 5 the uncertainty in [Be] may be of order 0.2 dex.

TABLE 5

COMPARISON BETWEEN PREDICTED AND OBSERVED SPALLOGENIC ABUNDANCES

Star (1)	[Fe/H] (2)	$[Be]_{obs}$ (3)	R_7/R_9 (4)	$[^7Li_{GCR}]$ (5)	$[^7Li_{obs}]$ (6)	$[^7Li_{obs} - {}^7Li_{GCR}]$ (7)	$[Li_p + {}^7Li_{GCR}]$ (8)
HD 134169	−1.0	0.65	16.2	1.86	2.21	1.95	>2.27
HD 76932	−1.1	0.78	19.1	2.06	1.96	...	>2.37
HD 84937	−2.1	< −0.8	147	<1.37	2.15	>2.07	2.15
HD 140283	−2.5	−1.0	362	1.56	2.05	1.88	>2.17

NOTES.—Col. (2): The first two are from RNBD; the last two are from Table 1, col. (4).

Col. (3): Li and Be abundances given as $12 + \log [N_{(Li\ or\ Be)}/N_H]$. HD 134169 and HD 84937 are from RNBD; HD 76932 is the average of RNBD and Boesgaard (1990); HD 140283 is the average of RNBD and Gilmore, Edvadsson, & Nissen, (1991). We have not listed previous (though pioneering) observations taken with the *IUE*, because of their coarser resolution and lower S/N. We have also not listed upper limits determined by Ryan et al. 1990.

Col. (4): From eqs. 7 and 8 of SW (see text, § 4).

Col. (6): Except for HD 84937, these are averages of the abundances compiled in DDK (Table 5). For HD 84937, we have taken into account the high-quality measurement of PHD (not listed in DDK) and other recent measurements (Deliyannis, Beers, & Ryan 1993), supporting an equivalent width between 23 and 25 mÅ; thus, the abundance 2.15 derived by B for 23 mÅ would appear to be a lower limit, which we adopt to be conservative (a lower Li abundance reduces the discrepancy discussed in text).

Col. (8): The expected total $[^7Li]$ in a star from adding the minimum Li_p derived from HD 84937, plus Li_{GCR}; to be compared with col. (6).

alone, particularly toward the turnoff, and would thus require early differential Galactic Li enrichment, perhaps independent of metallicity. However, the magnitude of the dispersion is also consistent with the predictions of evolutionary models of halo stars with rotation, which do not require (but do not rule out, either) early Galactic enrichment. These rotational models also predict a significant depletion in the lithium abundance during the stars' lifetime. If this is correct, then the standard model of BBN would no longer be self-consistent, and additional physics would be required (such as inhomogeneities or massive neutrinos). We emphasize that other causes of dispersion (e.g., such as differential Galactic Li enrichment, or perhaps only slight primordial inhomogeneities), and thus perhaps also a smaller Li depletion, cannot be ruled out.

In some cases, individual stellar reddenings must be considered in deriving the lithium abundances. The reddenings and temperatures of halo stars need to be determined by the most accurate means, preferably in more than one independent determination.

The rotational models predict that stars which formed with very low initial angular momentum will have lithium abundances measurably above the plateau. While such stars are expected to be relatively rare, and BD 23°3912 might be one of them, numerous new observations might discover some such stars. Such new observations would also allow a more thorough examination of the possibility of a lithium dispersion, and are important for testing the various arguments put forth in this paper. Finally, it may be worthwhile reducing the uncertainty in the equivalent width of some of the existing observations. In particular, 17 stars in Table 1 are limited to observations that have a derived 1 σ uncertainty greater than 2 mÅ, and for 15 of these stars only one observation exists. These stars are relatively bright, and it should be possible to easily obtain new measurements at many of today's observatories that can reduce the uncertainty to below 2 mÅ.

We are greatly indebted to L. Hobbs for suggesting the use of the color-W_{Li} plane, and to R. Rebolo for suggesting that we take into account the individual S/N and for pointing out the paper by R. Cayrel. We would also like to thank A. Boesgaard, C. Heller, L. Hobbs, P. Nissen, R. Rebolo, S. Ryan, D. Soderblom, F. Spite, and J. Thorburn for informative discussions and communications. This research was supported in part by NASA grants NAGW-777 and 778. C. P. D. gratefully acknowledges the support of the University of Hawaii Foundation, which aided in the completion of this project.

REFERENCES

Bessell, M. S., & Norris, J. 1982, ApJ, 263, L29
Boesgaard, A. M. 1985, PASP, 97, 784 (B)
———. 1990, in Sixth Cambridge Workshop: Cool Stars, Stellar Systems, and the Sun (ASP Conf. Ser., 9), ed. G. Wallerstein (Provo: Brigham Young), 317
Boesgaard, A. M. 1991, in The Formation and Evolution of Star Clusters (ASP Conf. Ser. 13), ed. K. Janes (Provo: Brigham Young), 463
Boesgaard, A. M., & Steigman, G. 1985, ARA&A, 23, 319
Burstein, D., & Heiles, C. 1982, AJ, 87, 1165
Carney, B. W. 1983, AJ, 88, 623
Cayrel, R. 1988, in IAU Symp. 132, The Impact of Very High S/N Spectroscopy on Stellar Physics, ed. G. Cayrel de Strobel & M. Spite (Dordrecht: Kluwer), 345
Chaboyer, B., Deliyannis, C. P., Demarque, P., Pinsonneault, M. H., & Sarajedini, A. 1992, ApJ, 388, 372
Conti, P. S., & Deutch, A. J. 1966, ApJ, 145, 742
Deliyannis, C. P. 1990, Ph.D. dissertation, Yale Univ.
Deliyannis, C. P., Beers, T. C., & Ryan, S. G. 1993, BAAS, in press
Deliyannis, C. P., & Demarque, P. 1991a, ApJ, 370, L89 (DD)
———. 1991b, ApJ, 379, 216
Deliyannis, C. P., Demarque, P., & Kawaler, S. D. 1990, ApJS, 73, 21 (DDK)
Deliyannis, C. P., Demarque, P., Kawaler, S. D., Krauss, L. M., & Romanelli, P. 1989, Phys. Rev. Lett., 62, 1583
Deliyannis, C. P., Demarque, P., & Pinsonneault, M. H. 1991, BAAS, 22, 1214
Deliyannis, C. P., & Pinsonneault, M. H. 1992, in Inside the Stars, ed. W. W. Weiss (ASP Conf. Ser., in press)
Endal, A. S., & Sofia, S. 1976, ApJ, 210, 184
———. 1978, ApJ, 220, 279
———. 1981, ApJ, 243, 625
Gilmore, G., Edvadsson, B., & Nissen, P. E. 1991, ApJ, 378, 17
Green, E. M., Demarque, P., & King, C. R. 1987, The Revised Yale Isochrones and Luminosity Functions (New Haven: Yale Univ. Observatory)
Hauck, B., & Mermilliod, M. 1985, A&AS, 60, 61
Hobbs, L. M., & Duncan, D. K. 1987, ApJ, 317, 796 (HD)
Hobbs, L. M., & Mathieu, R. D. 1991, PASP, 103, 431
Hobbs, L. M., & Pilachowski, C. 1988, ApJ, 326, L23 (HP)
Hobbs, L. M., & Thorburn, J. A. 1991, ApJ, 375, 116 (HT)
Hobbs, L. M., Welty, D. E., & Thorburn, J. A. 1991, ApJ, 373, L47
Ksawaler, S. D. 1987, PASP, 99, 1322
———. 1988, ApJ, 333, 236
Kraft, R. P. 1967, ApJ, 150, 551
Krauss, L. M., & Romanelli, P. 1990, ApJ, 358, 47
Laird, J. B., Carney, B. W., & Latham, D. W. 1988, AJ, 95, 1843
Magain, P. 1987, A&A, 181, 323
Malaney, R., & Mathews, G. J. 1991, preprint
Mathews, G. J., Alcock, C. R., & Fuller, G. M. 1990, ApJ, 349, 449
Maurice, E., Spite, F., & Spite, M. 1984, A&A, 132, 278

Michaud, G., Fontaine, G., & Beaudet, G. 1984, ApJ, 282, 206
Molaro, P. 1991, Mem. Soc. Astron. Ital. 62, 17
Nissen, P. E. 1988, A&A, 199, 146
Noyes, R. W., Weiss, N. O., & Vaughan, A. H. 1984, ApJ, 287, 769
Olsen, E. H. 1983, A&AS, 54, 55
Pagel, B. E. J. 1991, Nordita preprint, No. 91/18 A
Paresce, F. 1984, AJ, 89, 1022
Perrin, M.-N. 1986, A&A, 159, 239
Pilachowski, C., Hobbs, L. M., & De Young, D. S. 1989, ApJ, 345, L39 (PHD)
Pinsonneault, M. H., Deliyannis, C. P., & Demarque, P. 1992, ApJS, 78, 181 (PDD)
Pinsonneault, M. H., Demarque, P., Sofia, S., & Deliyannis, C. P. 1991, AAS, 22, 1206
Pinsonneault, M. H., Kawaler, S. D., & Demarque, P. 1990, ApJS, 74, 501
Pinsonneault, M. H., Kawaler, S. D., Sofia, S., & Demarque, P. 1989, ApJ, 338, 424
Proffitt, C. R., & Michaud, G. 1991, ApJ, 371, 584
Rebolo, R., Beckman, J. E., & Molaro, P. 1987, A&A, 172, L17 (RBM)
Rebolo, R., Molaro, P., & Beckman, J. E. 1988, A&A, 192, 192 (RMB)
Ryan, S. G., Bessell, M. S., Sutherland, R. S., & Norris, J. E. 1990, ApJ, 348, L57
Ryan, S. G., Norris, J. E., Bessell, M. S., & Deliyannis, C. P. 1992, ApJ, 388, 184 (RNBD)
Schuster, W. J., & Nissen, P. E. 1988, A&AS, 73, 225 (SN1)
———. 1989a, A&A, 221, 65 (SN2)
———. 1989b, A&A, 222, 69 (SN3)
Skumanich, A. 1972, ApJ, 171, 565
Soderblom, D. R., Oey, M. S., Johnson, D. R. H., & Stone, R. P. S. 1990, AJ, 99, 595
Sofia, S., Pinsonneault, M. H., & Deliyannis, C. P. 1991, in NATO Advanced Research Workshop, Angular Momentum Evolution of Young Stars, Noto, Italy, ed. S. Catalano & J. R. Stauffer (Dordrecht: Kluwer), 333
Spite, M., Maillard, J. P., & Spite, F. 1984, A&A, 141, 56 (SS2)
Spite, F., & Spite, M. 1982, A&A, 115, 357 (SS1)
———. 1986, A&A, 163, 140 (SS3)
Spite, M., Spite, F., Peterson, R. C., & Chaffee, F. H., Jr. 1987, A&A, 172, L9 (SSPC)
Steigman, G., & Walker, T. P. 1992, ApJ, 385, L13 (SW)
VandenBerg, D. A., & Bell, R. A. 1985, ApJS, 58, 561
Wagoner, R. V. 1973, ApJ, 179, 343
Yang, J., Turner, M. S., Steigman, G., Schramm, D. N., & Olive, K. A. 1984, ApJ, 281, 493